Selected chapters on astrophysics **Lecture 2**

¨Overview of recent advances in planetary migration: from theoretical models to high-resolution 3D multi-fluid simulations¨

PhD. Raúl O. Chametla

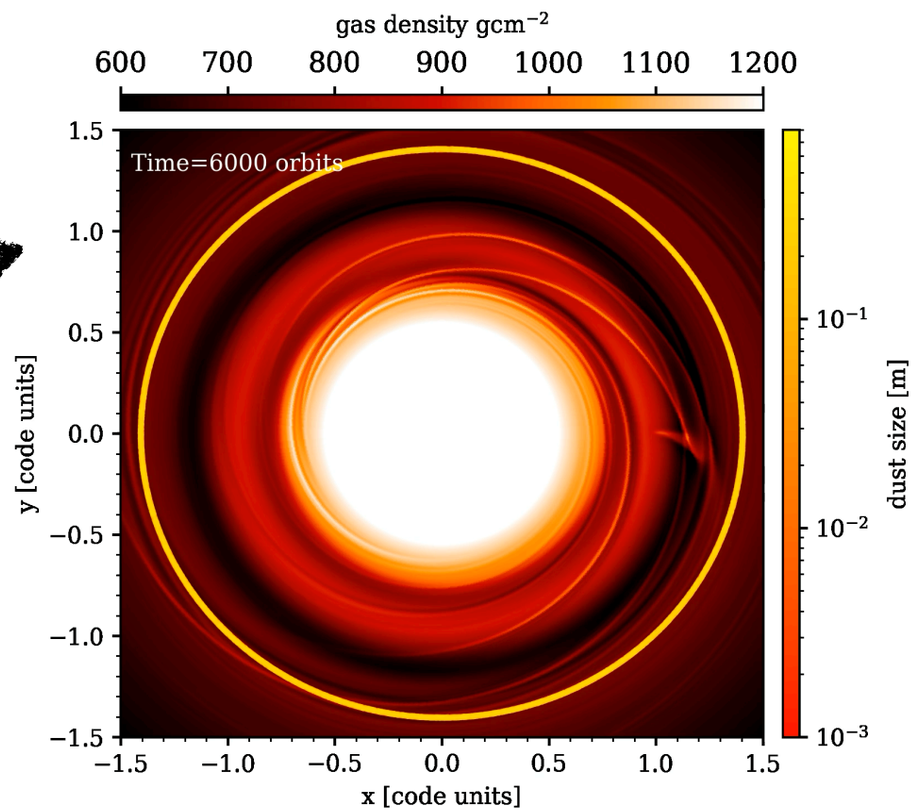

$$\Gamma_m = m\pi^2 \left(\frac{\Sigma_m}{r dD/dr} \left[r \frac{d\Phi_m}{dr} + \frac{2\Omega}{\Omega - \Omega_p} \Phi_m \right] \right)_{r=r_L}$$

$$D(r) = \kappa(r)^2 - m(\Omega_p - \Omega(r))$$

Migration runaway

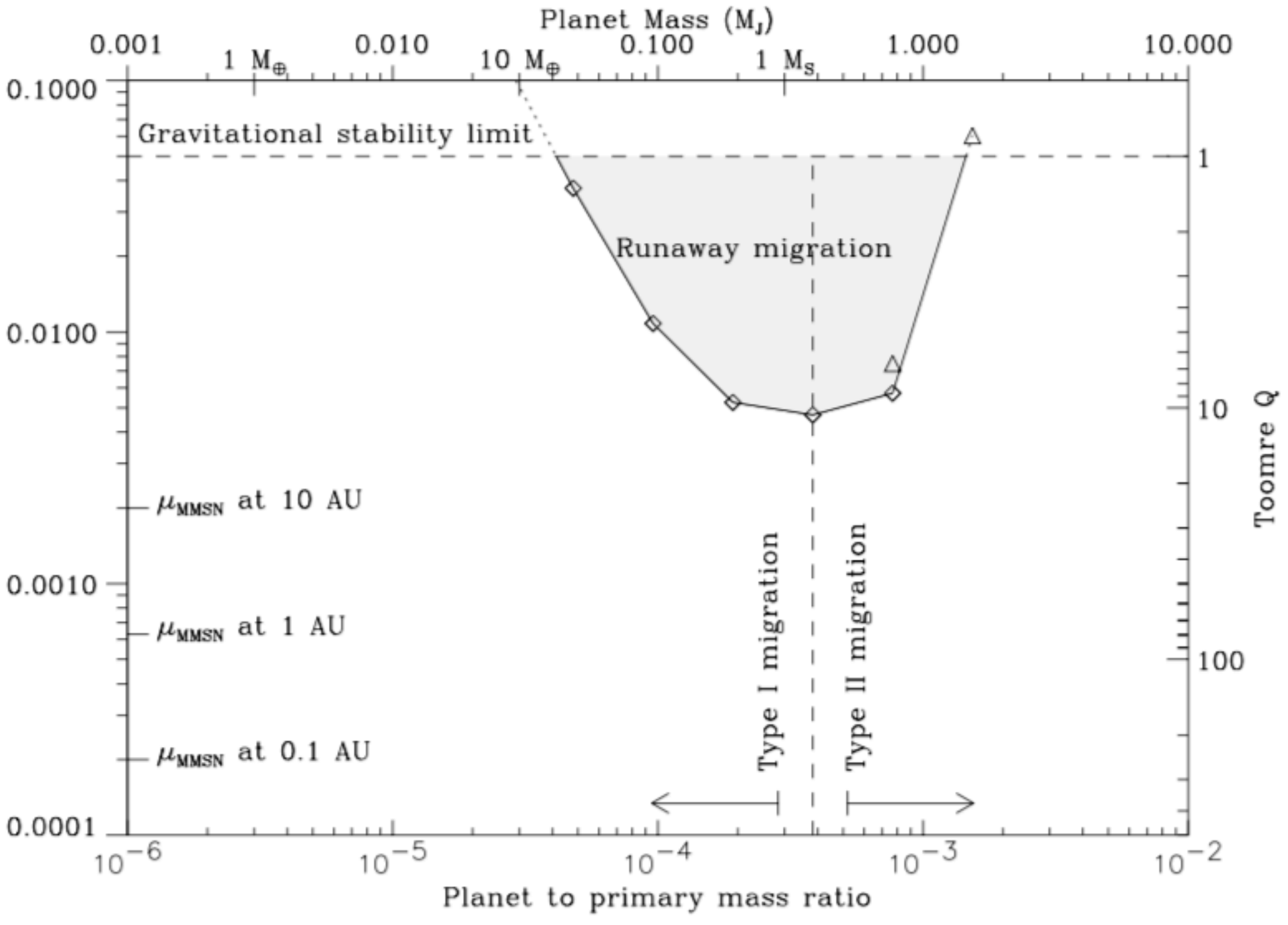
Planet Mass (M_J)
0.001
1 $M_\oplus$
0.010
10 $M_\oplus$
0.100
1 M_S
1.000
10.000
0.1000
0.0100
0.0010
0.0001
Gravitational stability limit
Runaway migration
μ_{MMSN} at 10 AU
μ_{MMSN} at 1 AU
μ_{MMSN} at 0.1 AU
Type I migration
Type II migration
1
10
100
Toomre Q
10^{-6}
10^{-5}
10^{-4}
10^{-3}
10^{-2}
Planet to primary mass ratio

The coorbital torque is assumed to come from orbit crossing fluid elements that exchange angular momentum with the planet when they execute a U-turn at the end of horseshoe streamlines.

When the planet migrates inward, the fluid elements of the inner disk undergo one such exchange as they pass to the outer disk.

The angular momentum they gain is removed from the planet, and this corresponds to a negative contribution to the corotation torque, which scales with the drift rate.

In addition, the material trapped in the coorbital region drifts radially with the planet, giving a positive contribution to the corotation torque, which also scales with the drift rate.

These two contributions do not cancel out if the coorbital region is depleted, in which case there is a net corotation torque that scales with the drift rate and the mass deficit in the coorbital region and has the same sign as the drift rate.

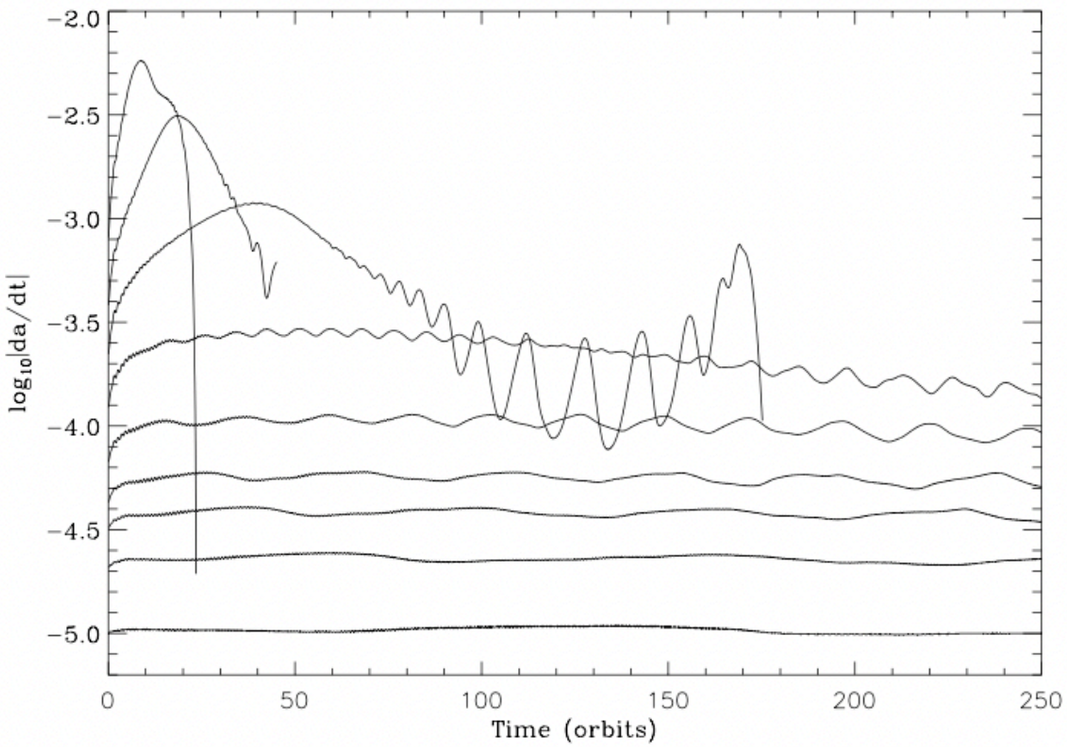

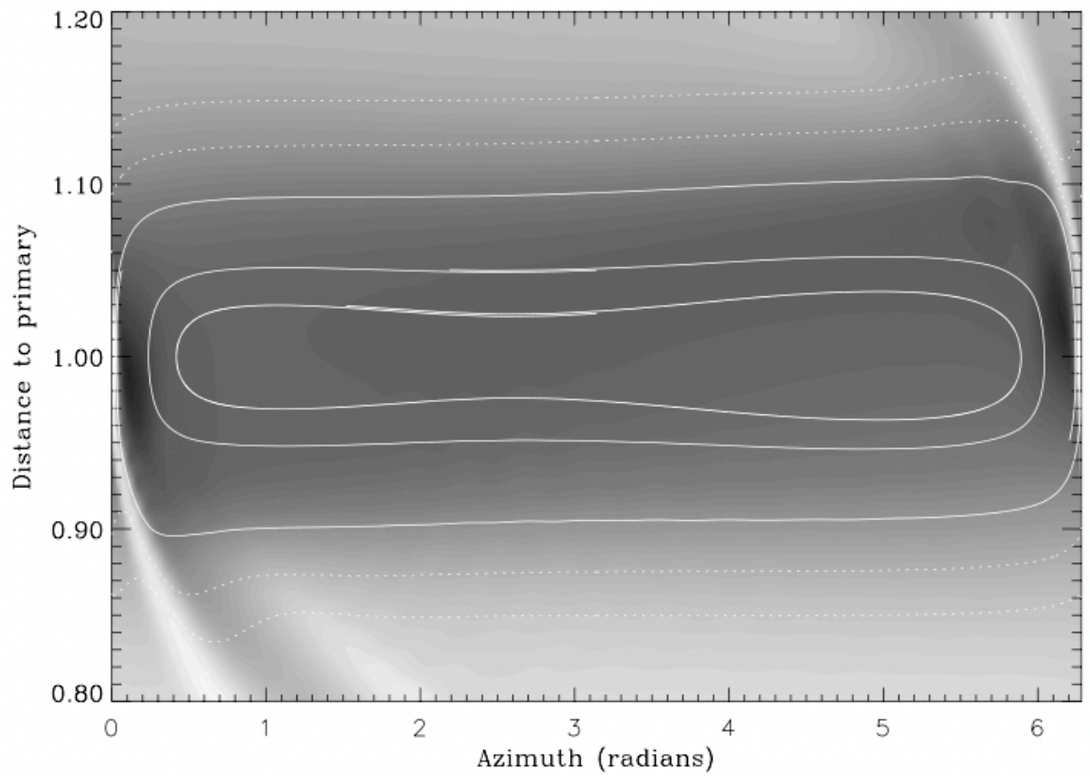

$$2Ba\dot{a}\tilde{M}_p = 2Ba\dot{a}\delta m + \Gamma_{\mathrm{LR}}$$

where $\tilde{M}_p = M_p + M_{\mathrm{cpd}}$ corresponds to an *effective* planet mass, and where $\delta m = 4\pi a x_s \Sigma_s - M_{\mathrm{hs}}$ is called the coorbital mass deficit.

This leads to a positive feedback on the migrating planet. In particular, if the coorbital mass deficit is larger than the planet mass, the migration rate undergoes a runaway that can vary the protoplanet semimajor axis by 50% over a few tens of orbits.

This can happen only if the planet mass is sufficient to create a dip or gap in its surrounding region and if the surrounding disk mass is larger than the planet mass.

This typically corresponds to planet masses in the sub-Saturnian to Jovian mass range embedded in massive protoplanetary disks.

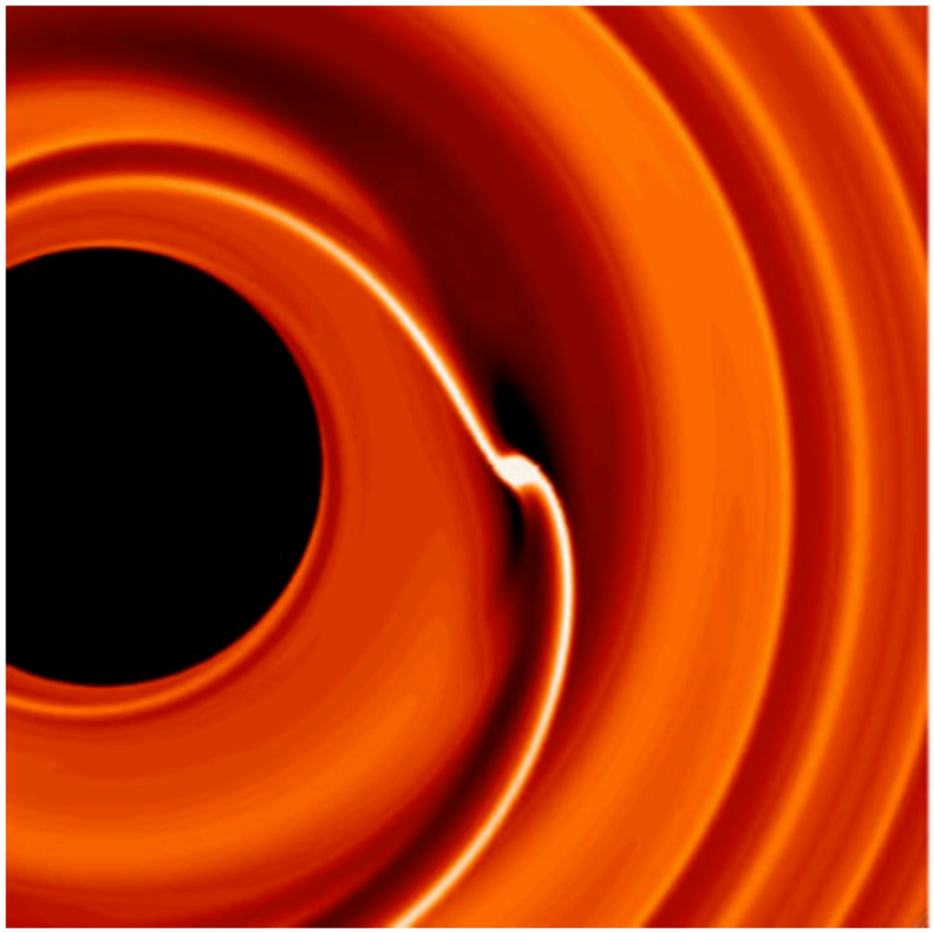

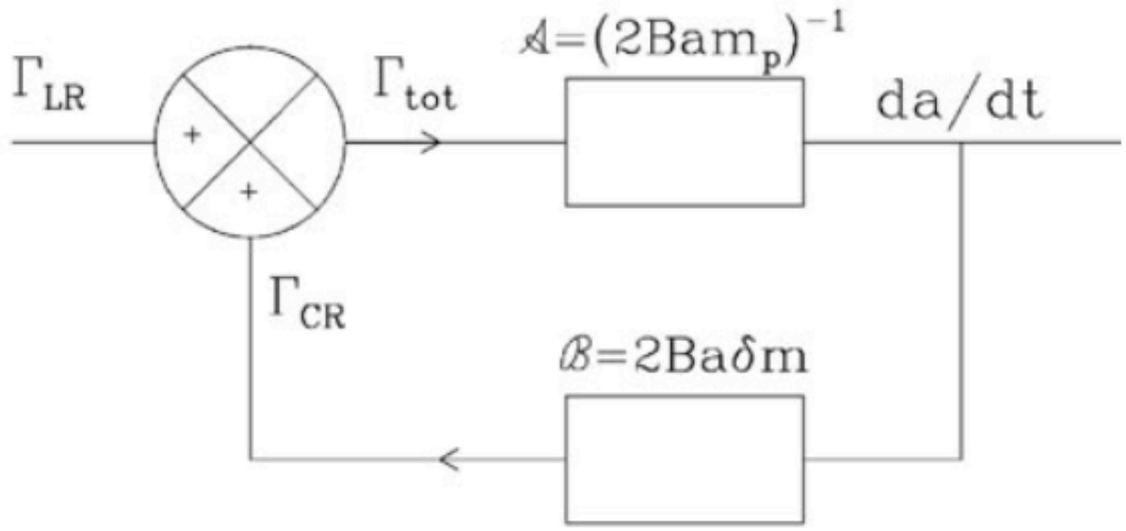

Fig. 6.14 *Left*: illustration of the flow asymmetry ahead of and behind a Saturn-mass planet undergoing rapid inward runaway migration. *Right*: type III planetary migration seen as a feedback loop. The latter remains stable if the open-loop transfer function $\mathscr{A} \times \mathscr{B} < 1$, or $\delta m < M_p$.

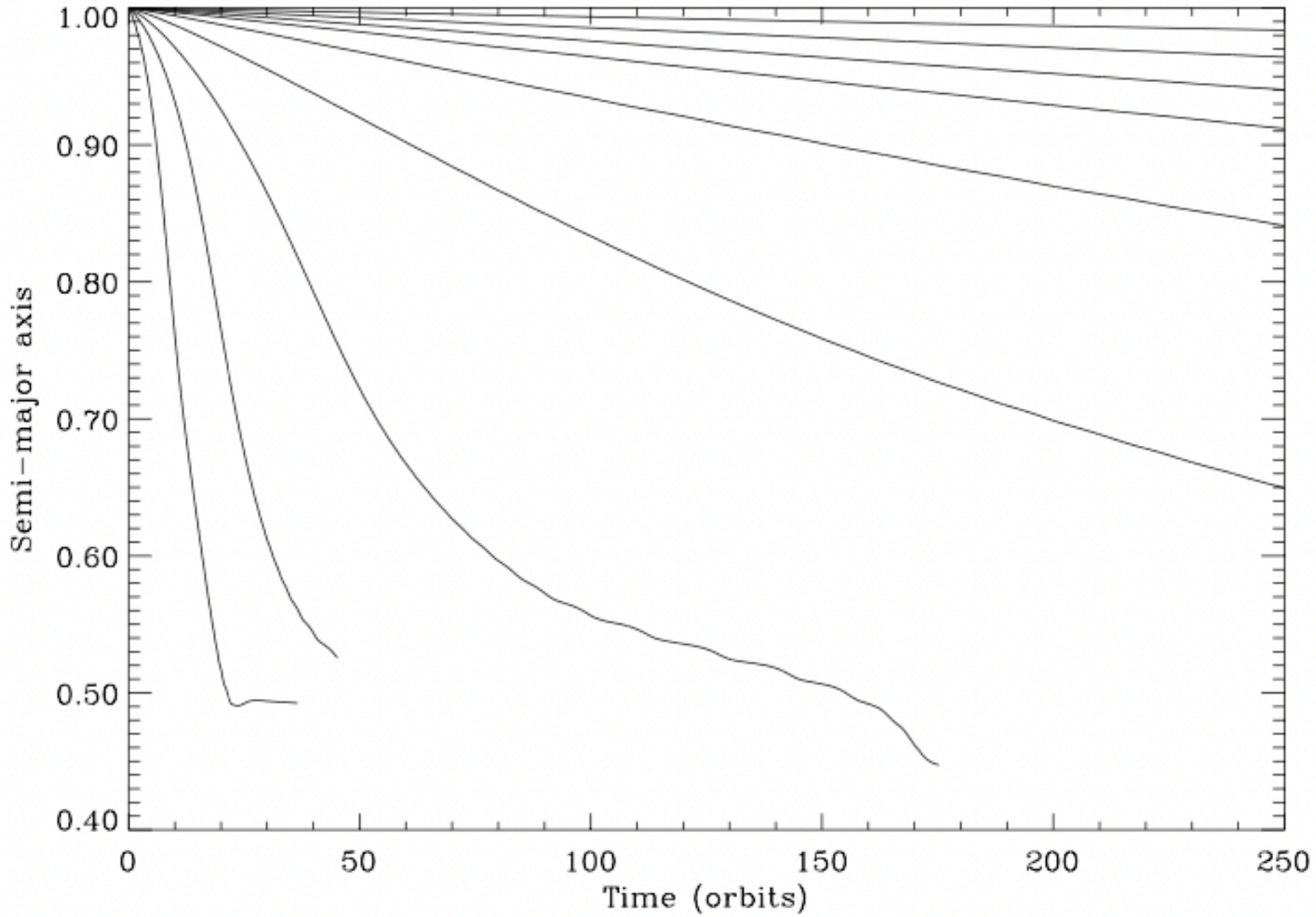

FIG. 2.—Semimajor axis as a function of time, for the different values of S_n, n ranging from 0 to 8 from top to bottom. The behavior is meaningless when a gets close to the grid inner boundary, located at $R_{\min} = 0.4$.

Runaway migration is a good candidate to account for the orbital characteristics of close orbiting giant planets, most of which have sub-Jovian masses.

Further, in the runaway regime, migration can be directed outward, which makes this regime potentially rich in a variety of important effects in shaping a planetary system during the last stages of its formation.

Numerical models on planetary migration

On the wake generated by a planet in a disk

For linear waves, any wave quantity X can be written in the form

$$X(r,\phi,t) = \mathrm{Re}\{\tilde{X}(r)\exp[\mathrm{i}\Phi_m(r,\phi,t)]\}, \quad (1)$$

where $\tilde{X}$ is an amplitude that varies slowly with r, while

$$\Phi_m = \int k(r)\,\mathrm{d}r + m(\phi - \Omega_\mathrm{p} t) \quad (2)$$

is a phase that varies rapidly with r. Here k is the radial wavenumber, which is real in regions of space where the wave propagates, and m is the azimuthal wavenumber.

Ogilvie & Lubow (2002)

$$\varphi = t + \frac{2}{3\epsilon}\left(r^{3/2} - \frac{3}{2}\ln r - 1\right).$$

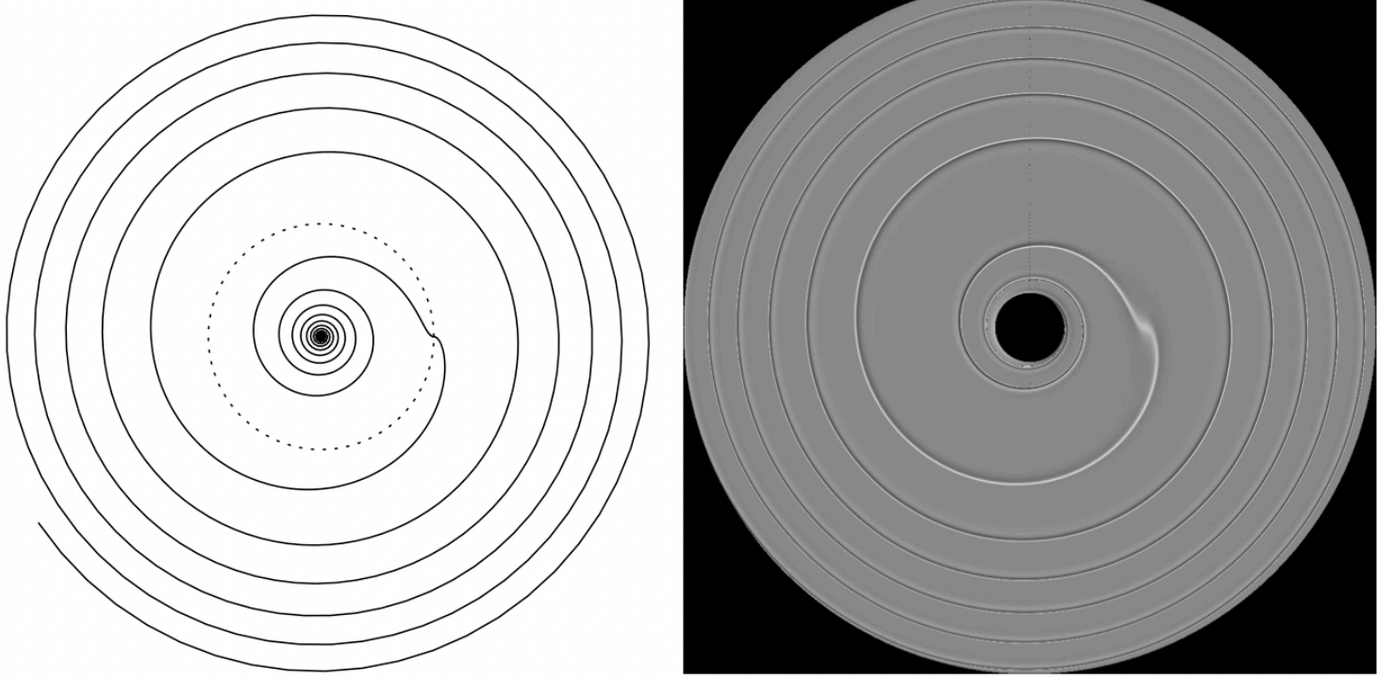

Figure 4. Left: Predicted shape of the spiral wake for $\epsilon = 0.05$, based on equations (13) and (24). The dotted line represents the corotation circle, $r = 1$. The planet is located at (1,0), and the outer radius plotted is $r = 3$. Right: Numerically calculated spiral wake for $\epsilon = 0.05$. The enthalpy perturbation is plotted using a linear grey-scale from negative (black) to positive (white). The maximum intensity corresponds to a fractional surface density perturbation, at $r = 1$, of $10^4(M_\mathrm{p}/M)$.

Two-dimensional disk model

The vertically integrated continuity equation

$$\frac{\partial \Sigma}{\partial t} + \nabla\cdot(\Sigma \boldsymbol{v}) = 0.$$

The components of the momentum equation are

$$\frac{\partial(\Sigma v_r)}{\partial t} + \nabla\cdot(\Sigma v_r \boldsymbol{v}) = \frac{\Sigma v_\phi^2}{r} - \frac{\partial P}{\partial r} - \Sigma\frac{\partial \Phi}{\partial r} + f_r,$$

$$\frac{\partial(\Sigma v_\phi)}{\partial t} + \nabla\cdot(\Sigma v_\phi \boldsymbol{v}) = -\frac{\Sigma v_r v_\phi}{r} - \frac{1}{r}\frac{\partial P}{\partial \phi} - \frac{\Sigma}{r}\frac{\partial \Phi}{\partial \phi} + f_\phi.$$

Here Σ denotes the surface density

$$\Sigma = \int_{-\infty}^{\infty} \rho\,\mathrm{d}z,$$

with ρ being the density, P the vertically integrated pressure, and f_r and f_ϕ the viscous force per unit area acting in the r and ϕ directions, respectively. The gravitational potential, Φ, is given by

$$\Phi = -\frac{GM*}{r} - \frac{Gm_\mathrm{p}}{\sqrt{r^2 + r_\mathrm{p}^2 - 2rr_\mathrm{p}\cos(\phi - \phi_\mathrm{p})}} + \frac{Gm_\mathrm{p}}{r_\mathrm{p}^3}\boldsymbol{r}\cdot\boldsymbol{r}_\mathrm{p} + G\int_\mathrm{S}\frac{\mathrm{d}m(\boldsymbol{r}')}{r'^3}\boldsymbol{r}\cdot\boldsymbol{r}', \quad (13)$$

where $M*$ and m_p are the masses of the central star and the protoplanet, respectively, and r_p and ϕ_p are the radial and azimuthal coordinates of the protoplanet.

Numerical models

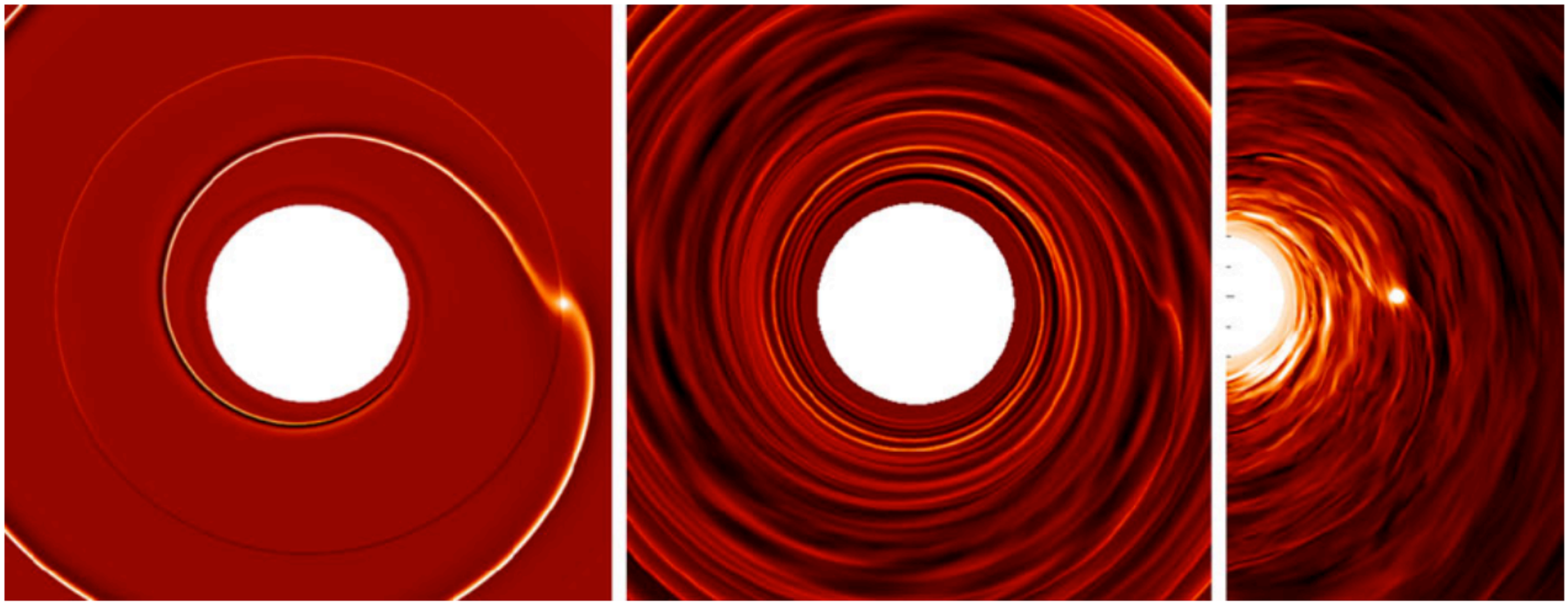

Fig. 6.12 Perturbation of the disc's density by an embedded planet. *Left*: adiabatic 2-dimensional disc. The density lobes within the coorbital region, which arise from the advection of entropy, help identify the (tiny) radial width of the planet's horseshoe region. *Middle*: case of an isothermal 2D disc with turbulence induced by stochastic stirring. *Right*: case of an isothermal 3D disc invaded by MHD turbulence due to the MRI (the density in the disc mid plane is displayed). In the *middle* and *right panels*, the turbulent density perturbation is comparable to the perturbed density associated to the planet's wakes.

Random walk migration in turbulent disks

There has been strong interest (e.g. Nelson & Papaloizou 2004, Uribe et al. 2011) in studying planet-disk interactions in turbulent disks, where the turbulence is magnetically generated by the magneto-rotational instability (MRI), instead of the laminar disks which we have used in the above analysis. Such laminar disks are strictly speaking not self-consistent, as they assume an abnormal viscosity (thought to be due to turbulence) without actually taking the consequence of turbulent motions into account.

More realistically, angular momentum transport itself derives from turbulence, which is accompanied by a spatially and temporally varying pattern of density fluctuations in the protoplanetary disk. These fluctuations will exert random torques on planets of any mass embedded within the disk.

In such turbulent disks, it is found that for low mass planets, Type I migration is no longer effective due to large fluctuations in the torque. The fluctuations in the torque created by the perturbations in the density can be larger than the mean torque expected for standard Type I migration in a laminar disk.

Uribe et al. (2011)

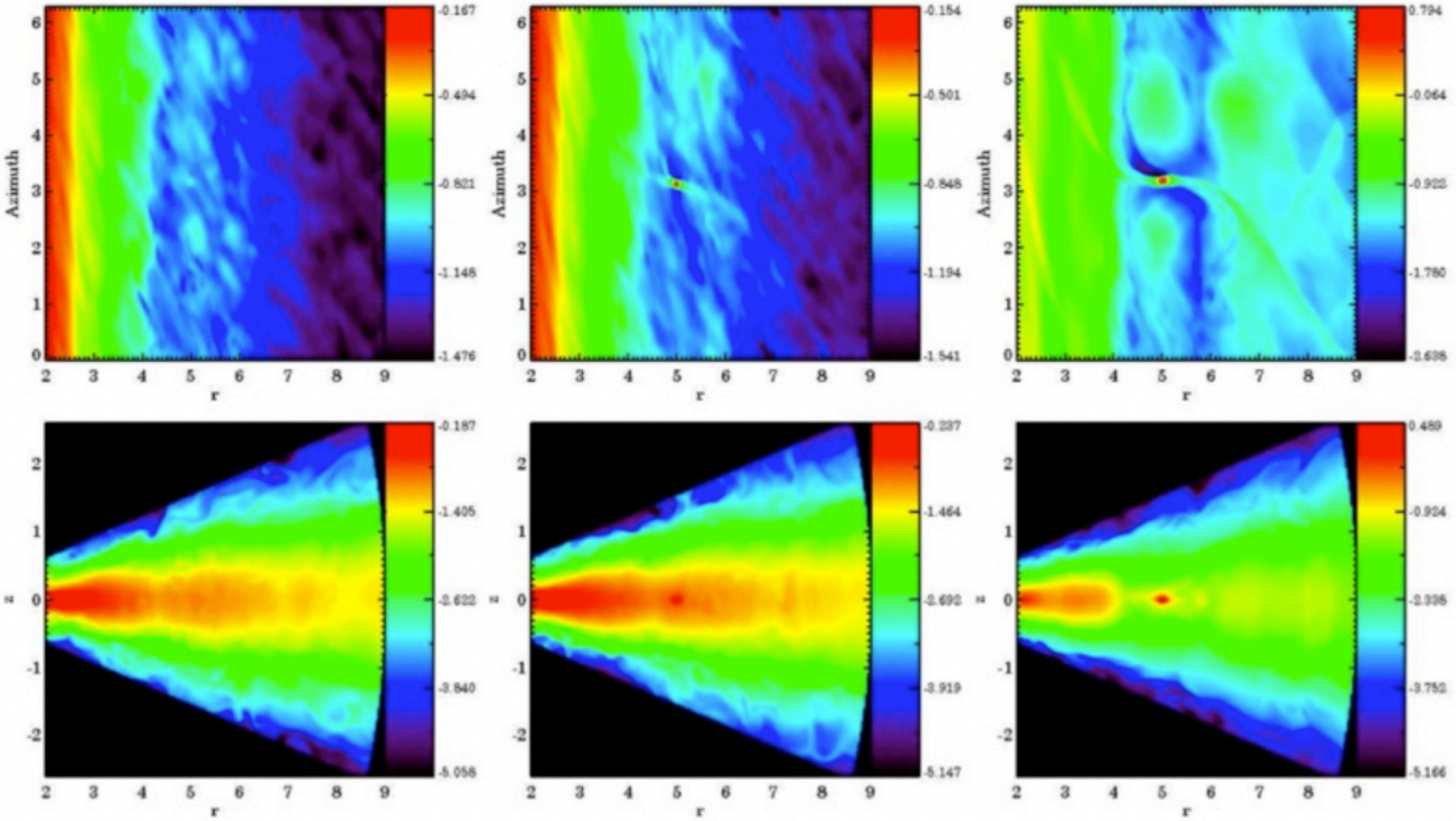

The plots show the logarithm of the disk density in the mid plane (top row) and in an azimuthal cut at the position of the planet (bottom row) for $q = 10^{-5}$ (~3 M_{earth}), $q = 10^{-4}$ (~30 M_{earth}) and $q = 10^{-3}$(~1 M_{Jup}). The left plot shows no significant perturbation of the density by the planet, and no spiral arms are seen, indicating that random torques are dominating.

Physical model (MHD case)

Magnetohydrodynamical equations describing the gas flow in 3D-MHD disks, considering a frame rotating with a uniform angular velocity $\mathbf{\Omega}$, are given by the equation of continuity

$$\frac{\partial \rho}{\partial t} = -(\mathbf{u}\cdot\nabla)\rho - \rho\nabla\cdot\mathbf{u}\,,$$

the gas momentum equation

$$\frac{\partial \mathbf{u}}{\partial t} = -(\mathbf{u}\cdot\nabla)\mathbf{u} - \frac{1}{\rho}\nabla p - \nabla\Phi + \frac{\mathbf{J}\times\mathbf{B}}{\rho} - \mathbf{\Omega}\times(\mathbf{\Omega}\times\mathbf{r}) - 2\mathbf{\Omega}\times\mathbf{u}\,,$$

and the induction equation

$$\frac{\partial \mathbf{B}}{\partial t} = \nabla\times\left[\mathbf{u}\times\mathbf{B} - \eta\mathbf{J}\right],$$

where ρ is the gas density, $\mathbf{u}$ is the gas velocity, Φ is the gravitational potential, and p is the pressure given as

$$p = \rho c_s^2\,,$$

with c_s the sound speed.

Table 2. Summary of Numerical Models in Section 3.

Disk model	Planet Mass $M_p[M_\oplus, M^*_{\rm Jup}]$	Orbit	Density slope q_ρ	Magnetic field plasma$-\beta$	Viscosity α-viscosity
α-disk					
AR1	$1M_\oplus$	Migrating	1.5	No	2.5×10^{-4}
AR2	$10M_\oplus$	Migrating	1.5	No	2.5×10^{-4}
AR2a	$10M_\oplus$	Migrating	0.5	No	2.5×10^{-4}
AR3	$30M_\oplus$	Migrating	1.5	No	2.5×10^{-4}
AR4	$100M_\oplus$	Migrating	1.5	No	2.5×10^{-4}
AR5	$1.05M_{\rm Jup}$	Fixed	1.5	No	2.5×10^{-4}
AR6	$3.15M_{\rm Jup}$	Fixed	1.5	No	2.5×10^{-4}
AR7	$10.5M_{\rm Jup}$	Fixed	1.5	No	2.5×10^{-4}
MHD-disk					
MR1	$1M_\oplus$	Migrating	1.5	10^3	No
MR2	$10M_\oplus$	Migrating	1.5	10^3	No
MR2a	$10M_\oplus$	Migrating	0.5	10^3	No
MR2b	$10M_\oplus$	Migrating	1.5	2×10^2	No
MR3	$30M_\oplus$	Migrating	1.5	10^3	No
MR4	$100M_\oplus$	Migrating	1.5	10^3	No
MR5	$1.05M_{\rm Jup}$	Fixed	1.5	10^3	No
MR6	$3.15M_{\rm Jup}$	Fixed	1.5	10^3	No
MR7	$10.5M_{\rm Jup}$	Fixed	1.5	10^3	No

NOTE—*Here $M_{\rm Jup} \equiv 318M_\oplus$ Earth masses.

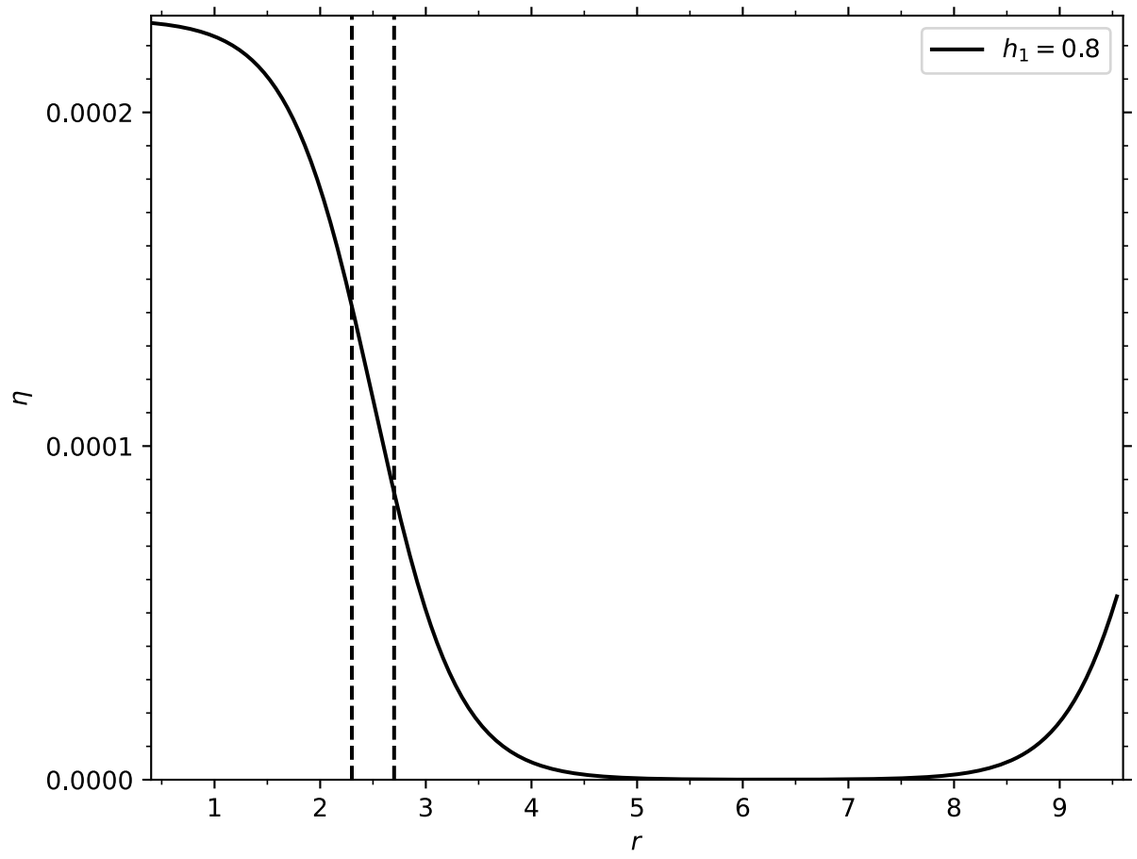

In the induction equation $\mathbf{J} = \mu_0^{-1} \nabla \times \mathbf{B}$, is the current density and η is the resistivity modeled as in Lyra et al. (2015):

$$\eta(r) = \eta_0 - \frac{\eta_0}{2}\left[\tanh\left(\frac{r - r_1}{h_1}\right) - \tanh\left(\frac{r - r_2}{h_2}\right)\right].$$

We use a reference frame centred on the star and rotating with the angular frequency $\mathbf{\Omega} = \Omega_p \hat{\mathbf{k}}$, where $\Omega_p \equiv \sqrt{GM_\star / r_p^3}$ is the angular velocity of the planet (with r_p the planet's orbital radius) and $\hat{\mathbf{k}}$ is a unit vector along the rotation axis. The gravitational potential Φ is given by

$$\Phi = \Phi_S + \Phi_p + \Phi_{\rm ind},$$

where

$$\Phi_S = -\frac{GM_\star}{r}, \qquad \Phi_p = -\frac{GM_p}{\sqrt{r'^2 + \epsilon^2}}, \qquad \Phi_{\rm ind} = \frac{GM_p}{r_p^3}\mathbf{r}\cdot\mathbf{r}_p + G\int_V \frac{dm(\mathbf{r}')}{r'^3}\mathbf{r}\cdot\mathbf{r}',$$

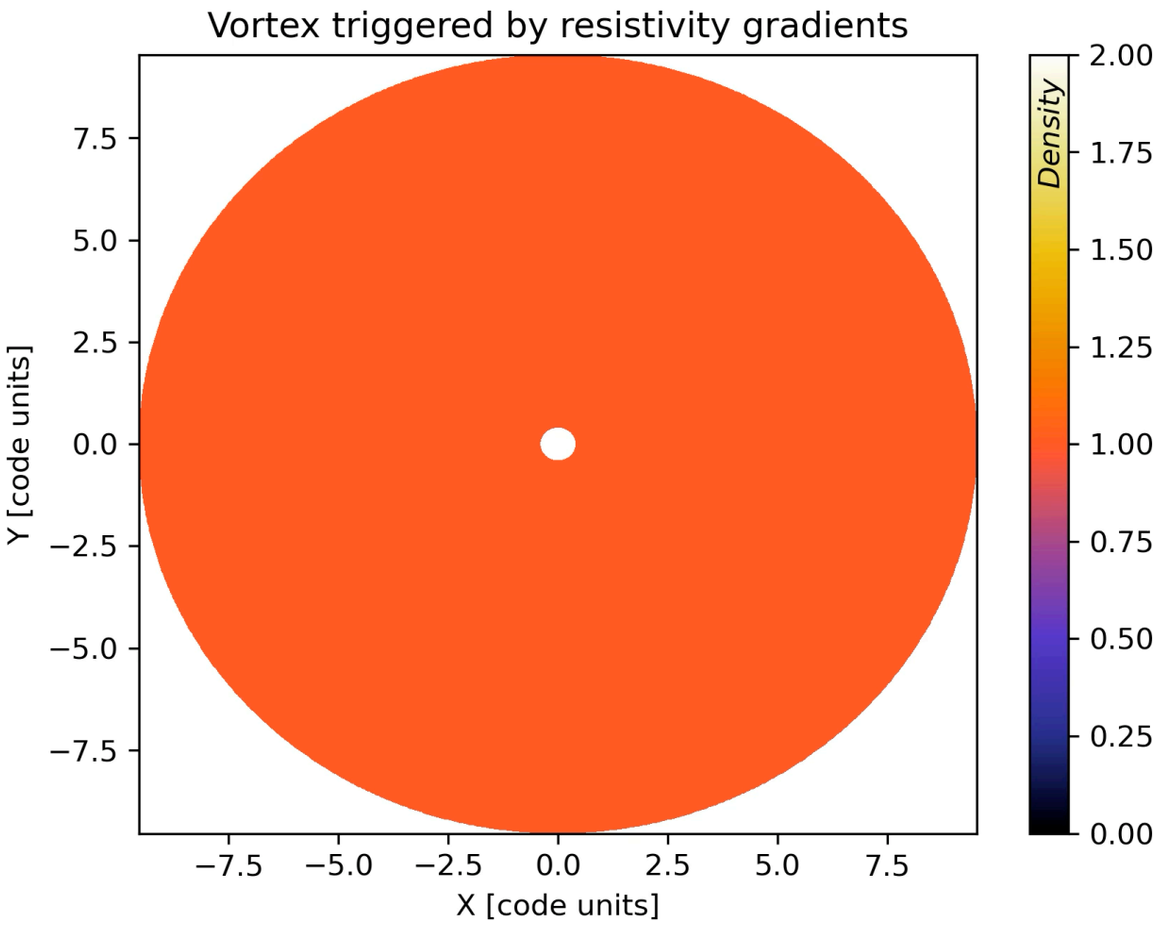
Vortex triggered by resistivity gradients
Y [code units]
X [code units]
Density
7.5
5.0
2.5
0.0
−2.5
−5.0
−7.5
2.00
1.75
1.50
1.25
1.00
0.75
0.50
0.25
0.00

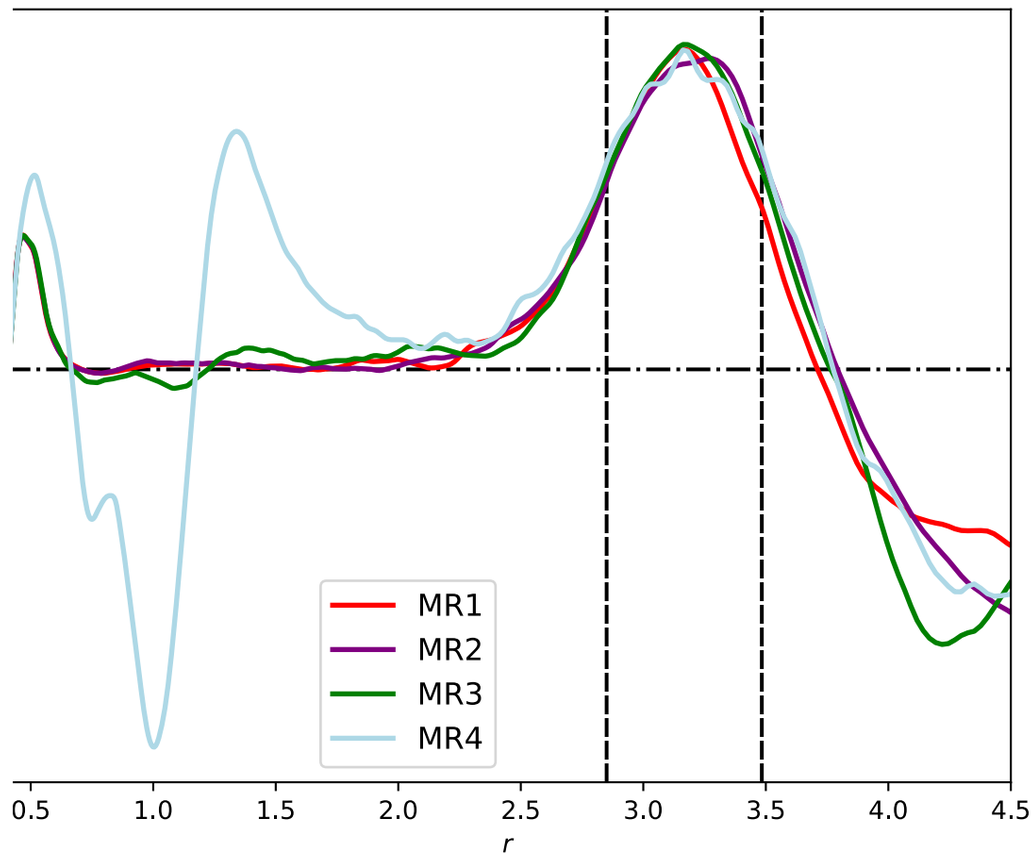
MR1
MR2
MR3
MR4
0.5
1.0
1.5
2.0
2.5
3.0
3.5
4.0
4.5
r

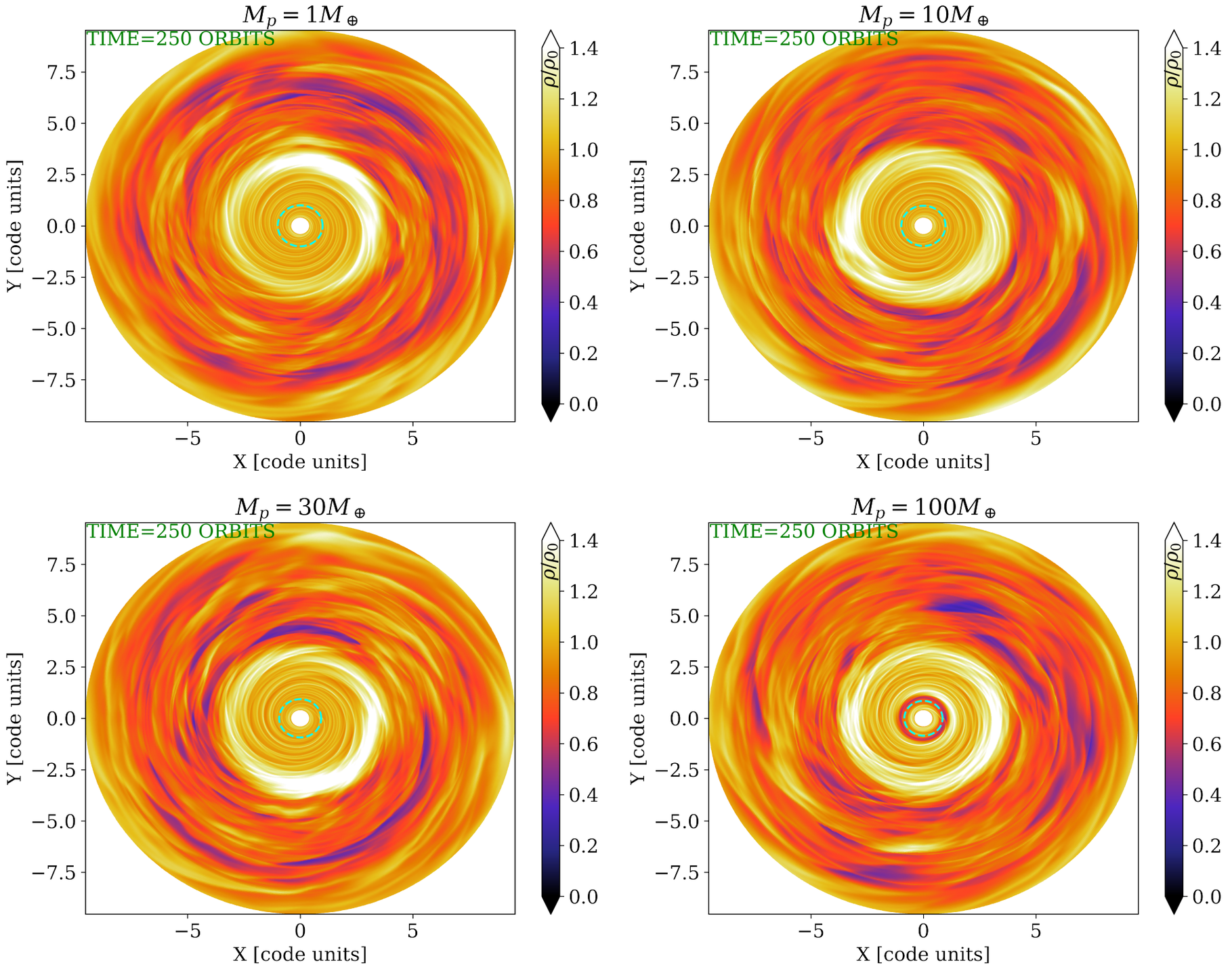
$M_p = 1M_\oplus$
TIME=250 ORBITS
$M_p = 10M_\oplus$
TIME=250 ORBITS
$M_p = 30M_\oplus$
TIME=250 ORBITS
$M_p = 100M_\oplus$
TIME=250 ORBITS
Y [code units]
X [code units]
ρ/ρ_0
7.5
5.0
2.5
0.0
−2.5
−5.0
−7.5
−5
0
5
1.4
1.2
1.0
0.8
0.6
0.4
0.2
0.0

Fast inward migration

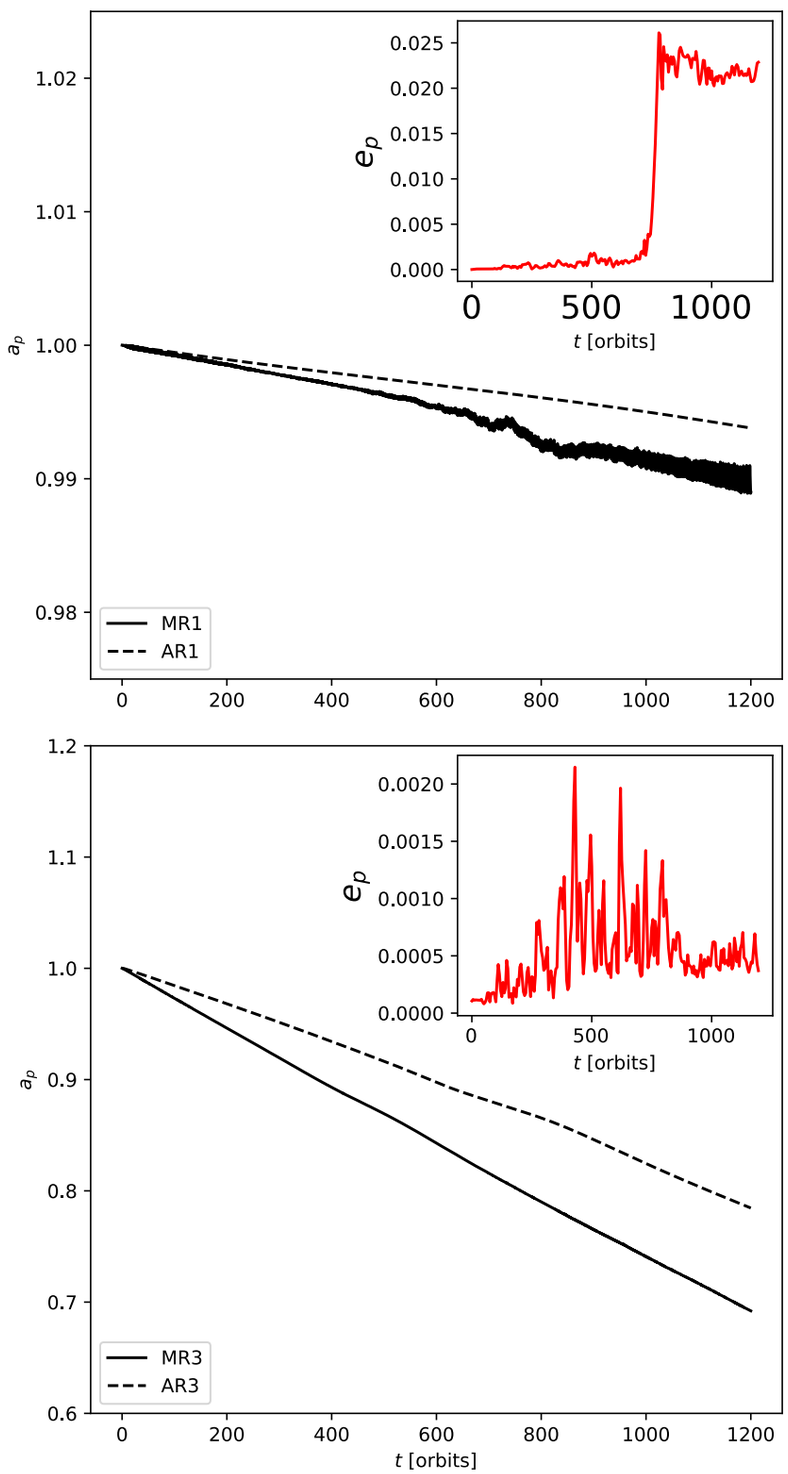

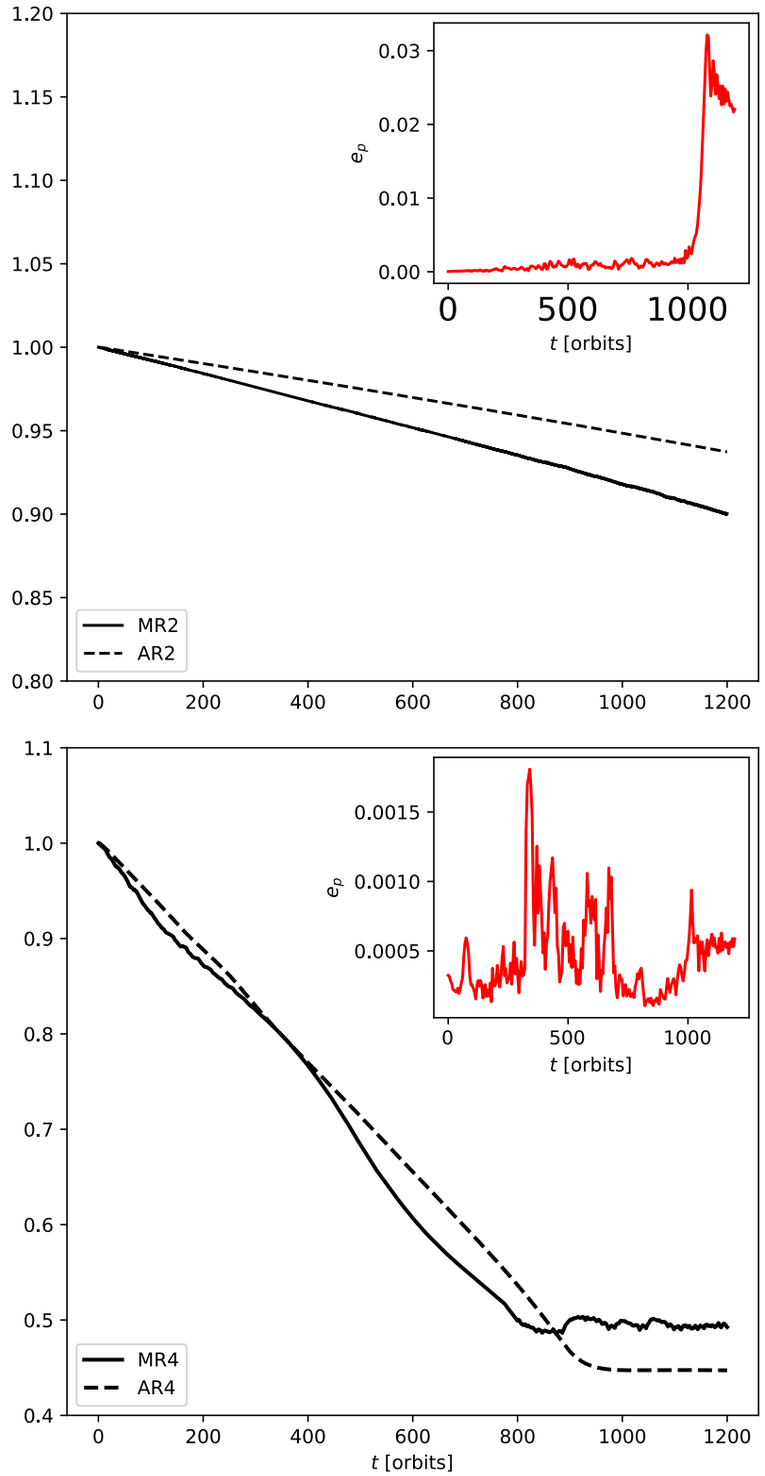

Fast inward migration

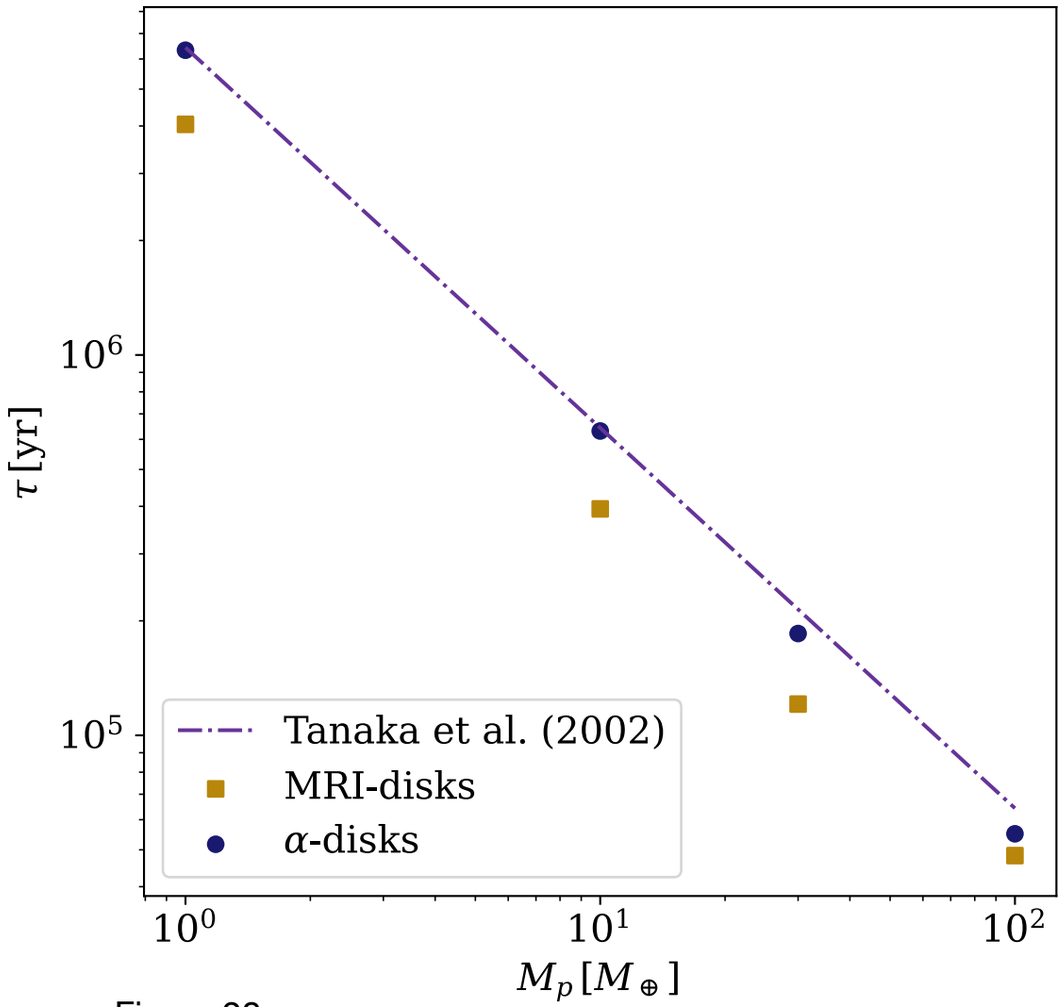

Figure 28.

For a locally isothermal 3D disk, with a power-law surface density profile, the total torque (Lindblad plus corotation), Γ, acting on a planet was estimated by Tanaka et al. (2002). They found that

$$\Gamma = (1.364 + 0.541 q_\rho)\Gamma_0,$$

where $\Gamma_0 \equiv (M_p/M_\star)^2 (r_p \Omega_p / c_s)^2 \Sigma_p r_p^4 \Omega_p^2$.

From this equation, the type I radial migration speed of the planet can be calculated from the conservation of angular momentum, as

$$\frac{dr_p}{dt} = 2 r_p \frac{\Gamma}{L_p},$$

with $L_p = M_p \sqrt{G M_\star r_p}$ the planet's angular momentum.

Therefore, the migration timescale is given as

$$\tau = (2.7 + 1.1 q_\rho)^{-1} M_p r_p^2 \Omega_p \Gamma_0^{-1}\,.$$

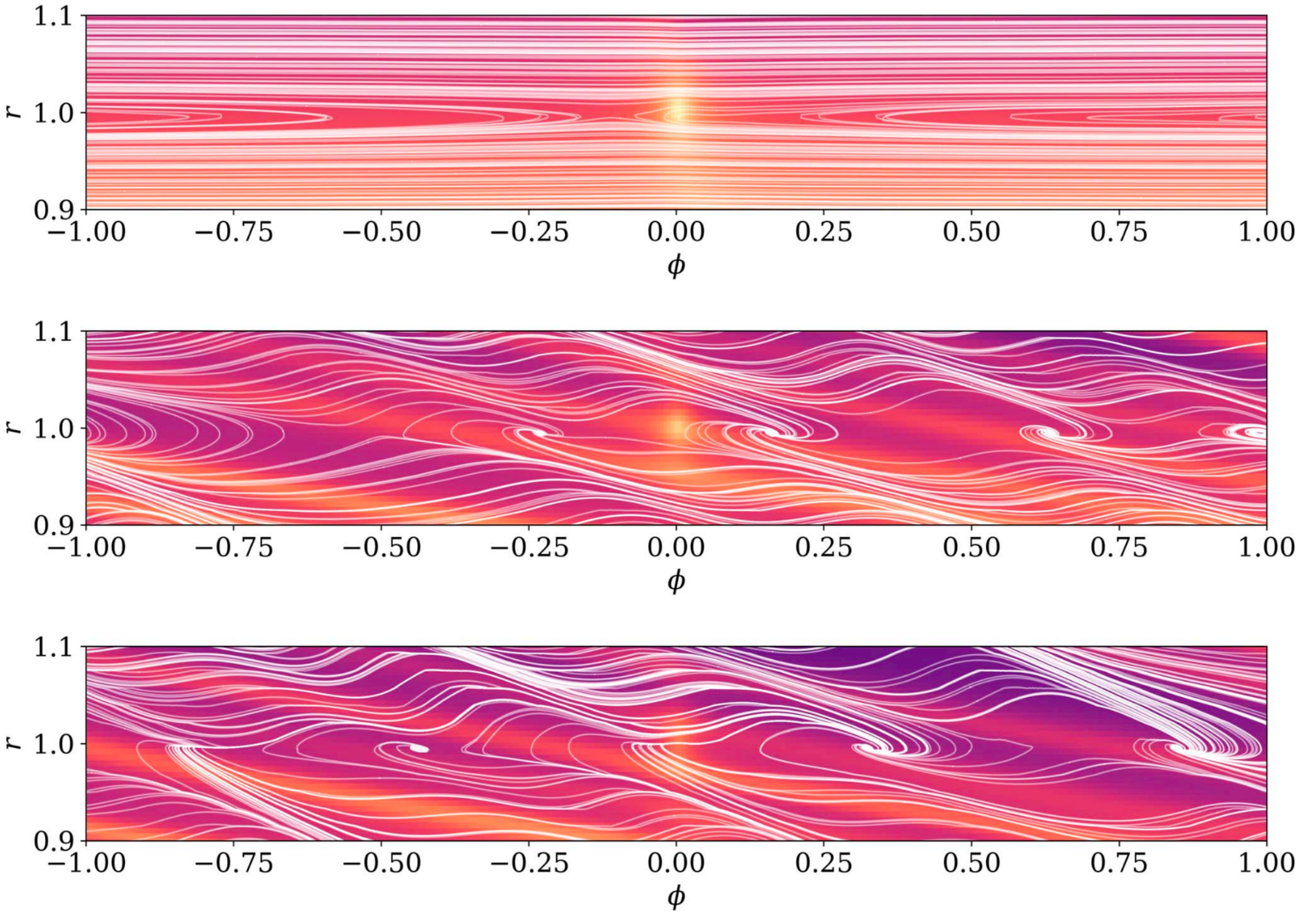

Figure 13. Streamlines overplotted in the gas density at the midplane for the MR2a model calculated at $t = 5$, $t = 60$, and $t = 80$ orbits (top, middle and bottom panels, respectively).

Non-isothermal migration

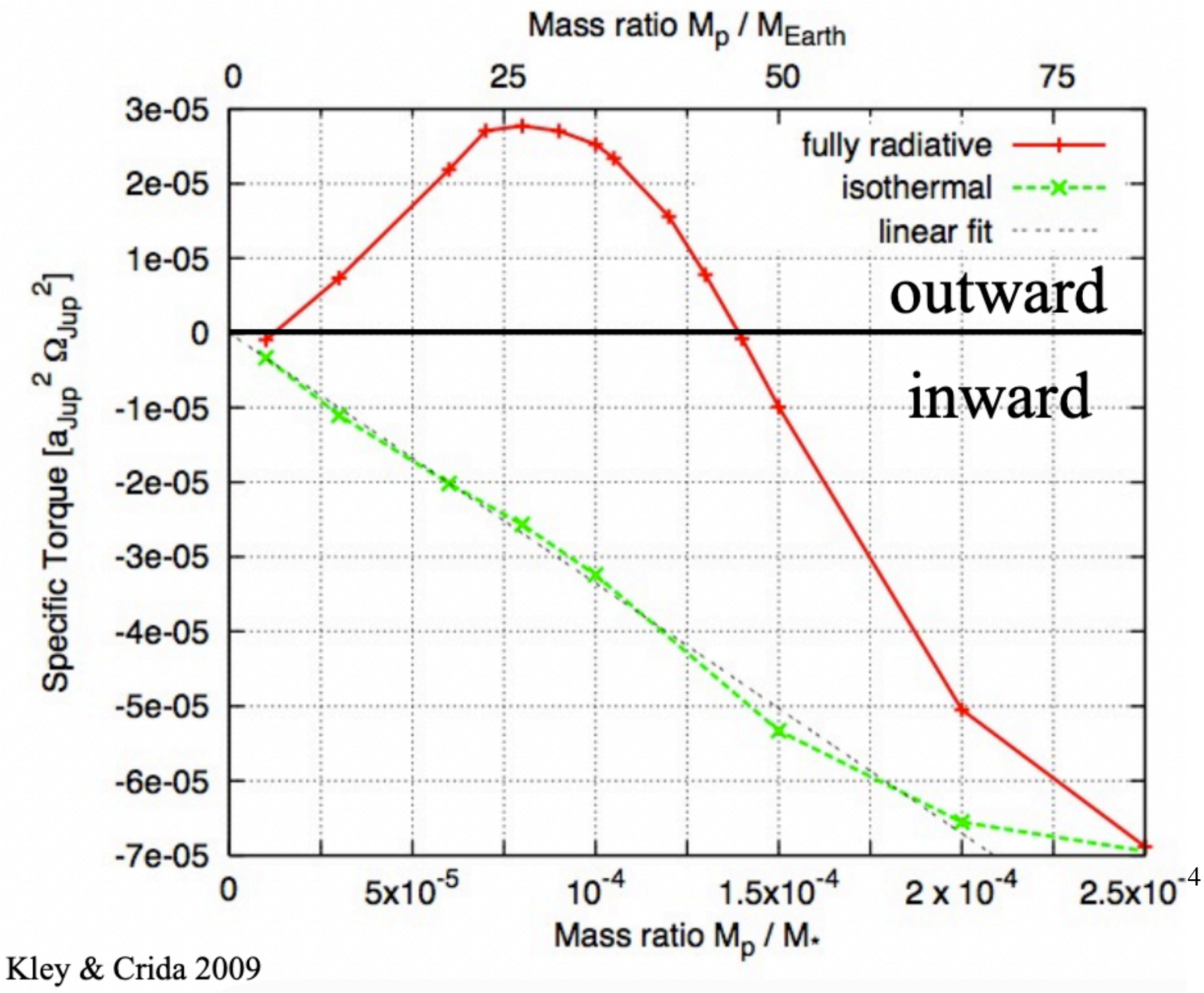

Kley & Crida 2009

Radiation hydrodynamic simulations treating correctly the energy transport in the disk find that below a certain threshold mass, migration can be directed outwards, due to a different density distribution around the planet.

Migration of Earth-sized planets in 3D radiative discs

Cold thermal Torques

The motion of the gas is described by the Navier–Stokes equations in a rotating frame in spherical coordinates as follows.

(i) Continuity equation:

$$\frac{\partial \rho}{\partial t} + \nabla \cdot (\rho \boldsymbol{v}) = 0,$$

where ρ is the density of the gas and $v = (v_r, v_\varphi, v_\theta)$ the velocity, with $v_\varphi = r \sin(\theta)(\omega + \Omega)$, where ω is the azimuthal angular velocity in the rotating frame.

(ii) Equations for the momenta. The Navier–Stokes equations for the radial momentum $J_r = \rho v_r$, the polar momentum $J_\theta = \rho r v_\theta$ and the angular momentum $J_\varphi = \rho r \sin(\theta) v_\varphi = \rho r^2 \sin^2\theta(\omega + \Omega)$ read

$$\begin{cases} \frac{\partial J_r}{\partial t} + \nabla \cdot (J_r \boldsymbol{v}) = \rho[\frac{v_\theta^2}{r} + \frac{v_\varphi^2}{r} - \frac{\partial \Phi}{\partial r} \\ \qquad\qquad + \frac{1}{\rho}(f_r - \frac{\partial P}{\partial r})] \\ \frac{\partial J_\theta}{\partial t} + \nabla \cdot (J_\theta \boldsymbol{v}) = \rho r[\frac{v_\varphi^2 \cot(\theta)}{r} - \frac{1}{r}\frac{\partial \Phi}{\partial \theta} \\ \qquad\qquad + \frac{1}{\rho}(f_\theta - \frac{1}{r}\frac{\partial P}{\partial \theta})] \\ \frac{\partial J_\varphi}{\partial t} + \nabla \cdot (J_\varphi \boldsymbol{v}) = \rho r \sin(\theta)[-\frac{1}{r\sin\theta}\frac{\partial \Phi}{\partial \varphi} \\ \qquad\qquad + \frac{1}{\rho}(f_\varphi - \frac{1}{r\sin\theta}\frac{\partial P}{\partial \varphi})]. \end{cases}$$

The function $f = (f_r, f_\varphi, f_\theta)$ is the divergence of the stress tensor (see, for example, Tassoul 1978). The potential Φ acting on the disc consists of the contribution of the star $\Phi_* = -GM_*/r$ and planets Φ_p, plus indirect terms that arise from the primary acceleration due to the planets and discs gravity.

To the usual Navier–Stokes equations, they add the equations for the internal energy modeled as in Kley et al. (2009):

$$\begin{cases} \frac{\partial E}{\partial t} + \nabla \cdot (E\boldsymbol{v}) = -p\nabla \cdot \boldsymbol{v} + Q^{+} \\ \qquad\qquad\qquad\qquad -\nabla \cdot D\nabla T \\ D = -\frac{\lambda c 4 a_{\mathrm{r}} T^{3}}{\rho \kappa} \end{cases}, \tag{3}$$

where E is the internal energy $E = \rho c_{\mathrm{v}} T$, T is the temperature of the disc and c_{v} is the specific heat at constant volume. On the right-hand side, the first term denotes the compressional heating, Q^{+} the expression for the viscous heating and $D\nabla T$ is the radiative flux.

The system of equations is closed using an ideal gas EOS: $P = R_{\mathrm{gas}} \rho T/\mu$ with mean molecular weight $\mu = 2.3(\mathrm{g\,mol^{-1}})$ for standard solar mixture. Taking into account that

$$E = R_{\mathrm{gas}} \rho T/\mu(\gamma - 1),$$

this relates to the pressure as

$$P = E(\gamma - 1).$$

Lega et al. (2014)

Table 1. Simulations parameters.

Mass ($M_\oplus$)	$(N_r, N_\theta, N_\varphi)$	$\alpha_{\rm sm}$	n cells in x_{hs}
10	(254, 42, 754)	0.5	4
5	(262, 32, 768)	0.5	3
5	(359, 50, 1068)	0.5	4
3	(350, 42, 1025)	0.5	3
3	(464, 60, 1382)	0.7	4
3	(464, 60, 1382)	0.5	4
3	(464, 60, 1382)	0.3	4
3	(464, 60, 1382)	0.1	4
3	(580, 90, 1727)	0.5	5
2	(568, 90, 1696)	0.5	4

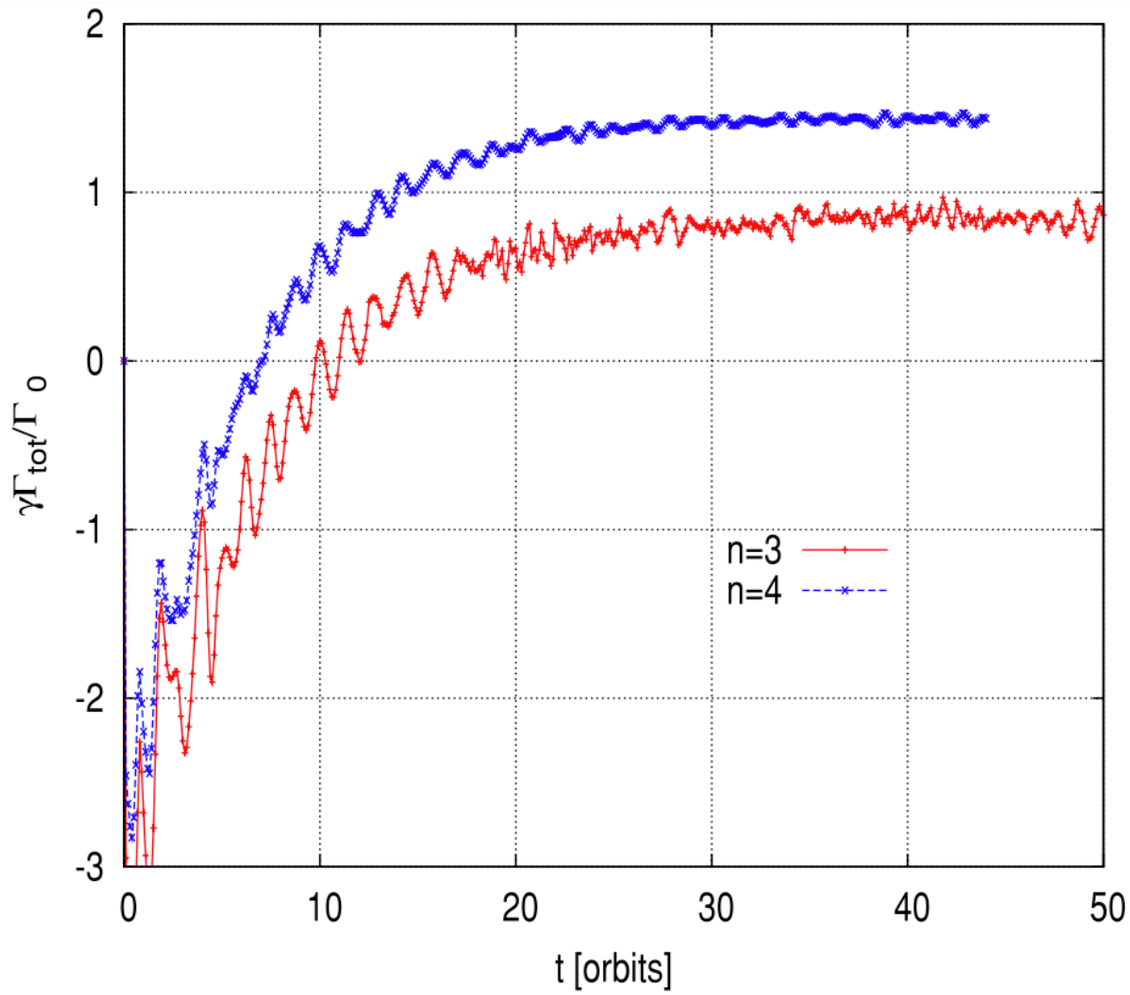

Figure 1. Evolution of the total torque with time for a planet of 5 $M_\oplus$ and two different resolutions corresponding to $n = 3$ and 4 cells in the horseshoe region.

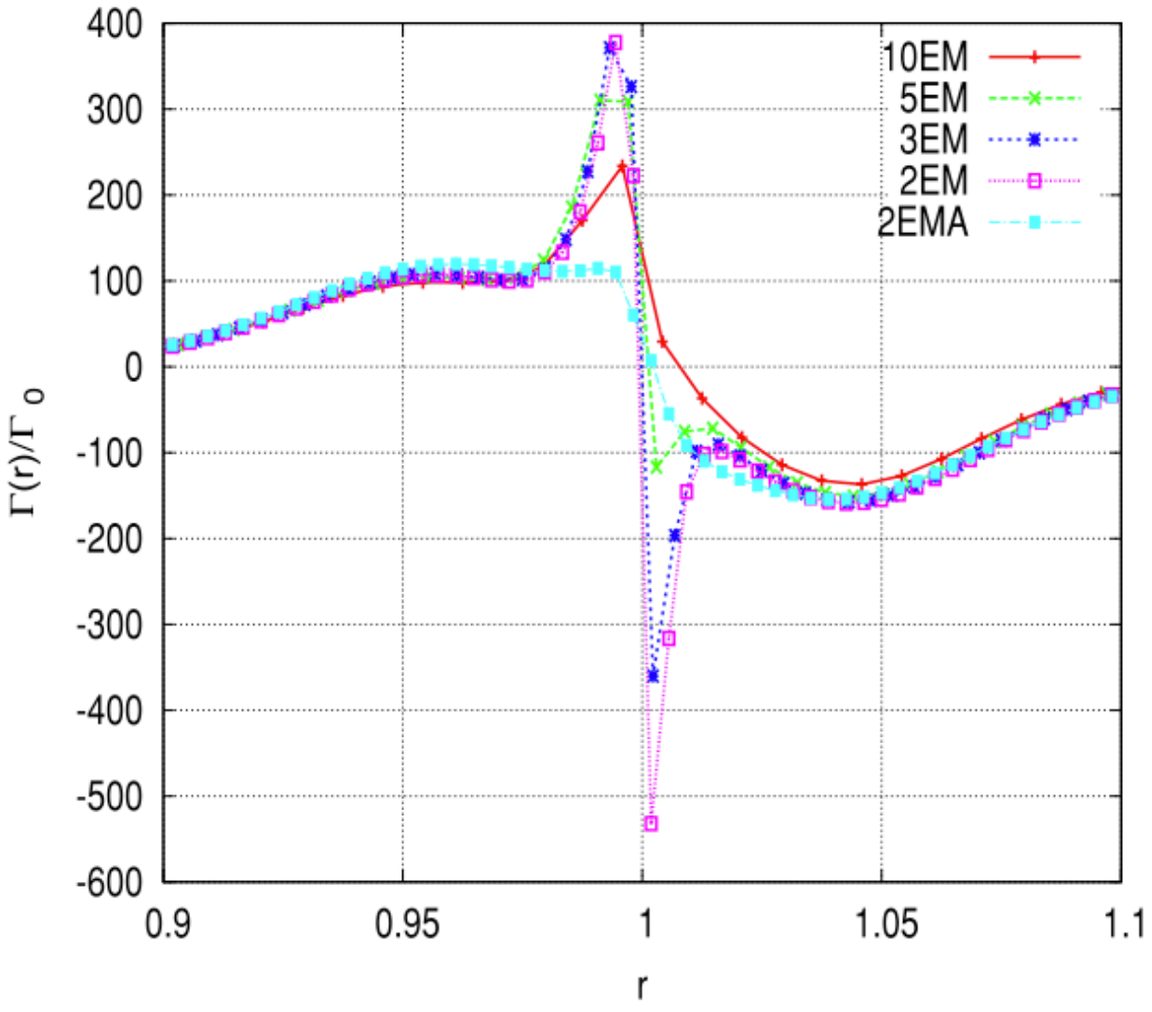

Figure 5. Radial torque density normalized with respect to Γ_0. The Lindblad torque scales with the square of the mass ratio q, while unexpected contributions come from the close vicinity of the planets for $m_p < 10\,M_\oplus$. For comparison the radial torque density obtained for an adiabatic simulation is shown.

(i) The Lindblad torque scales as expected (Goldreich & Tremaine 1980; Paardekooper et al. 2010) with Γ_0, i.e. with the square of the mass ratio q.

(ii) Compared with the adiabatic case, where the component of the corotation torque due to the temperature gradient saturates, we notice that the total torque acting on a $M_p = 10M_\oplus$ has a positive contribution just inside $r = 1$; also a small torque excess is observed for $r > 1$.

Both features are expected (Paardekooper & Mellema 2006) in radiative discs as a result of the heating and cooling process of the gas librating in the horseshoe region leading to a positive total torque.

(iii) The corotation torque is expected to scale with Γ_0. At $r < 1$, we observe a positive spike due to the entropy-related part of the corotation torque (non-linear contribution or horseshoe drag).

(iv) A new and totally unexpected feature appears for $r > 1$. We observe a negative spike which is not seen for $M_p \geq 10M_\oplus$

(v) The positive and negative spikes contributions appear to be asymmetric, the negative spike providing a larger contribution which is responsible for the negative total torque, i.e. for the transi- tion from outward to inward migration.

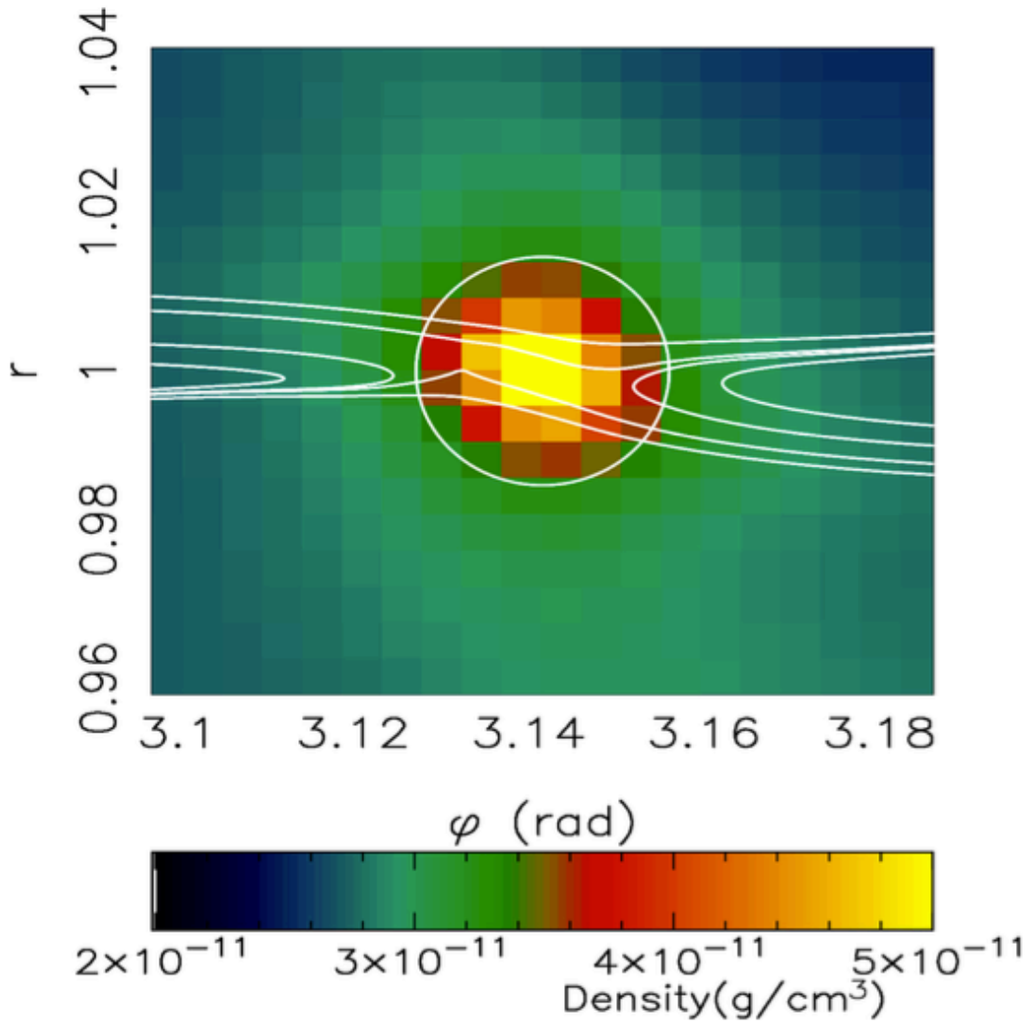

Figure 10. Mid-plane density field for a $3\,M_\oplus$ planet (resolution $n = 4$, $\alpha_{sm} = 0.5$).

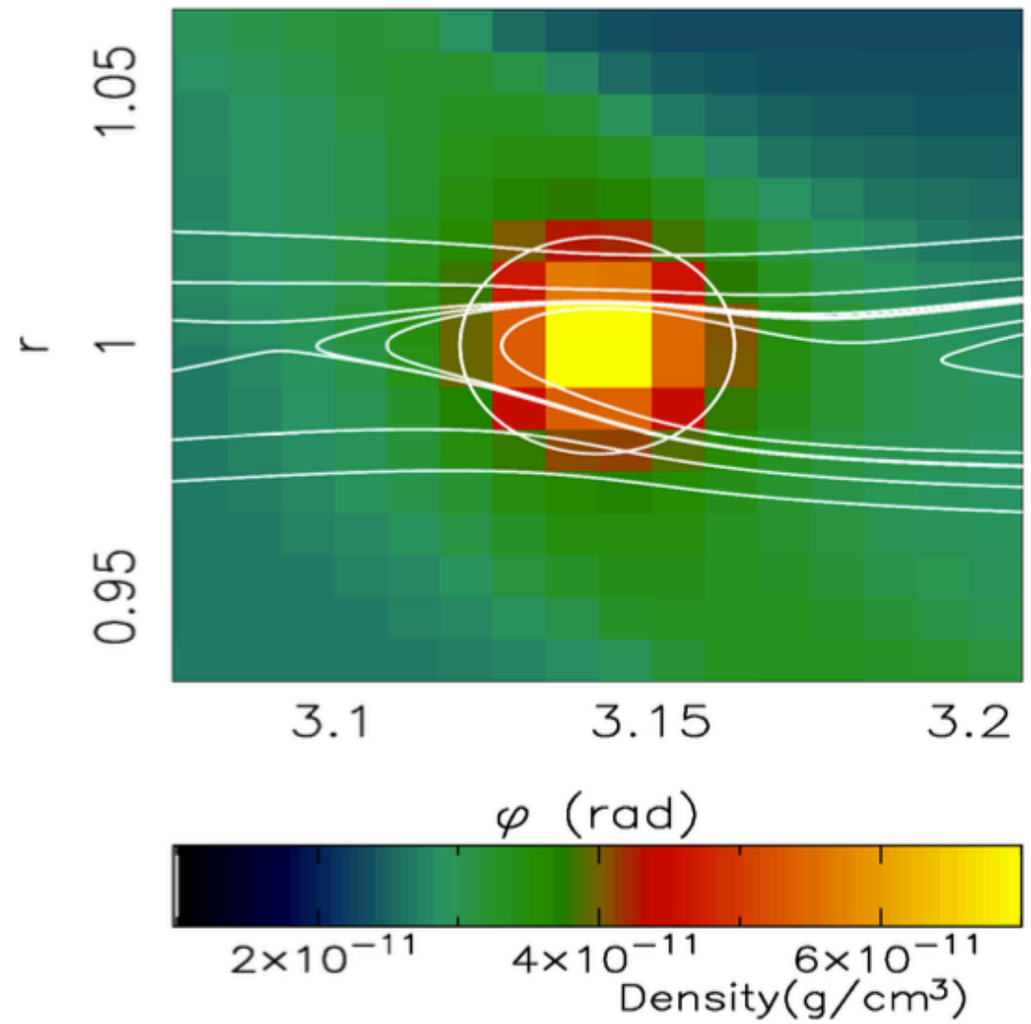

Figure 12. Mid-plane density field for a $10\,M_\oplus$ planet (resolution $n = 4$, $\alpha_{sm} = 0.5$).

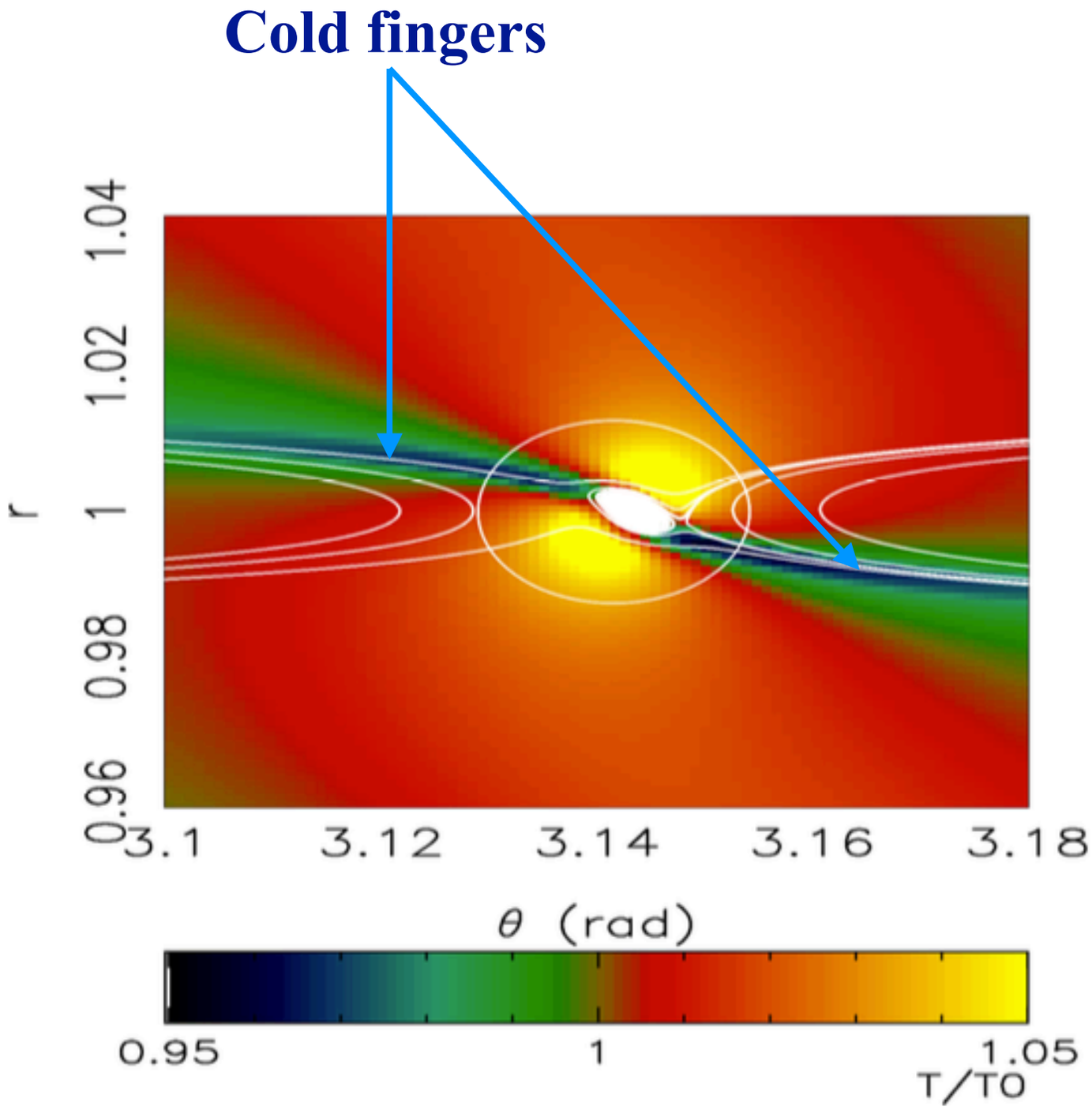

Figure 18. 2D simulation: perturbed temperature around a $2\,M_{\oplus}$ planet after 60 orbits for a simulation in which the gas has Keplerian speed, the surface density and the temperature are initially constant with respect to r.

Planet heating prevents inward migration of planetary cores

Hot thermal torques

Benitez-Llambay et al. (2015)

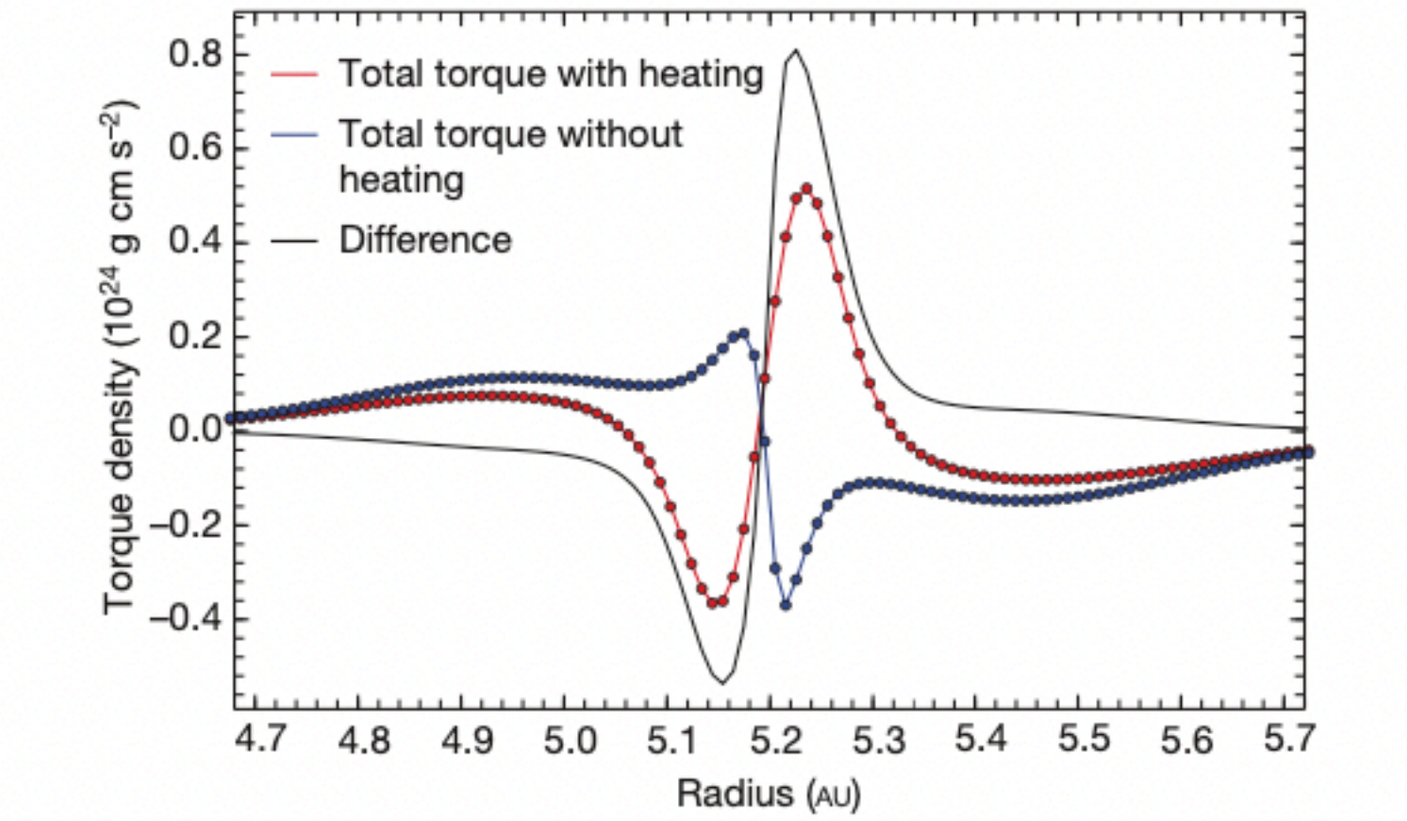

Figure 1 | Comparison of the torques in the cases with and without heating. The blue curve shows the torque radial density (that is, torque exerted by rings of unitary radial width upon the planet) in the non-heating case and the red curve when the heating is included. Their difference shows the heating torque density (black). This calculation corresponds to an embryo planet of $3M_{\oplus}$ that is located at 5.2 AU from its central star.

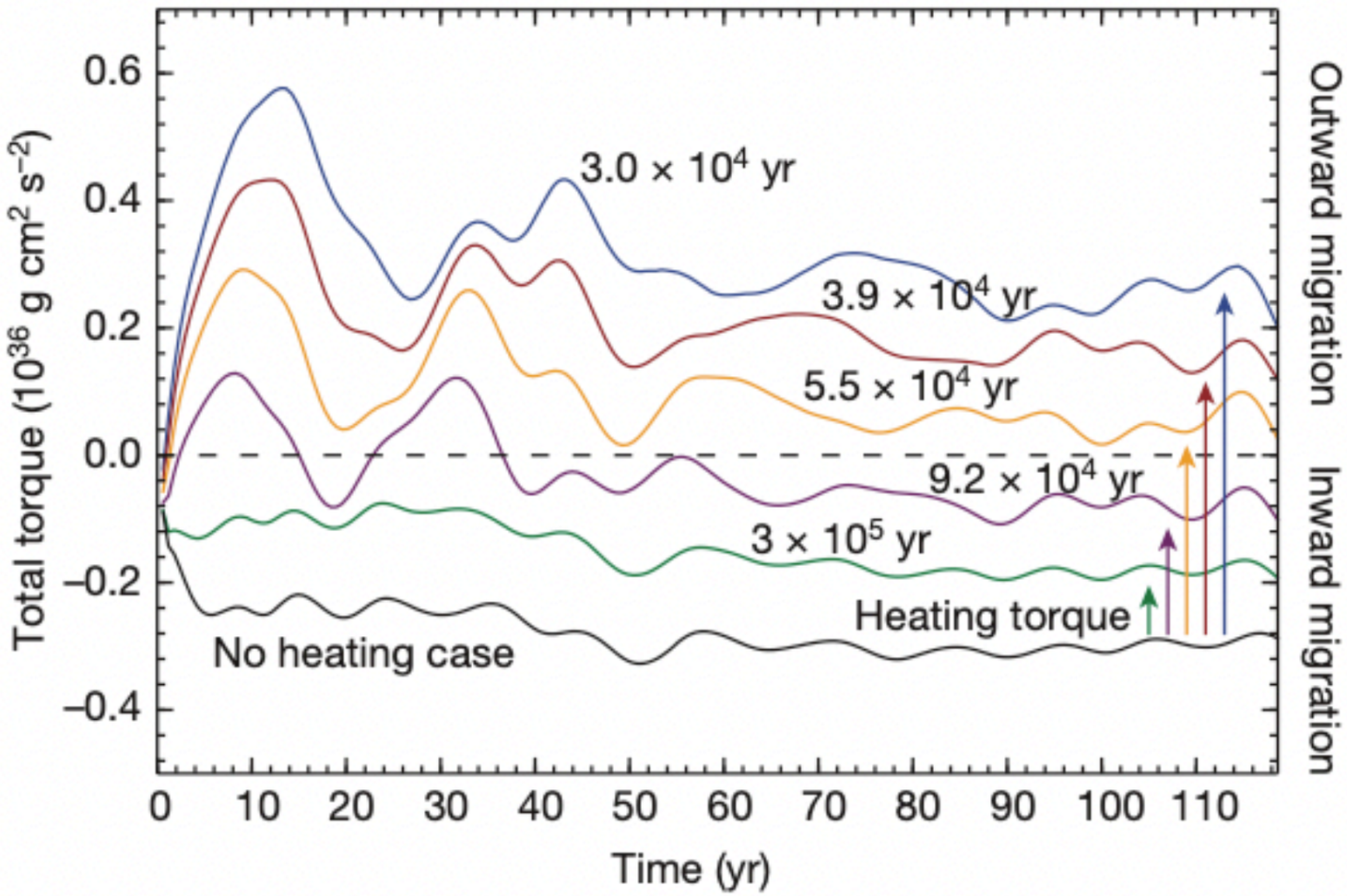

Figure 2 | Heating torque for different growth timescales. The curves are labelled with the planetary mass-doubling time (that is, the time it takes the accreting planet to double its mass) and show the torque exerted on an embryo planet of $3M_\oplus$ over the first 118 years of our calculation (ten orbits). With low or no heating, the planet migrates inward while for larger rates (mass doubling time shorter than 92,000 years) it migrates outward. The dashed line corresponds to no migration. The vertical arrows show the magnitude of the heating torque.

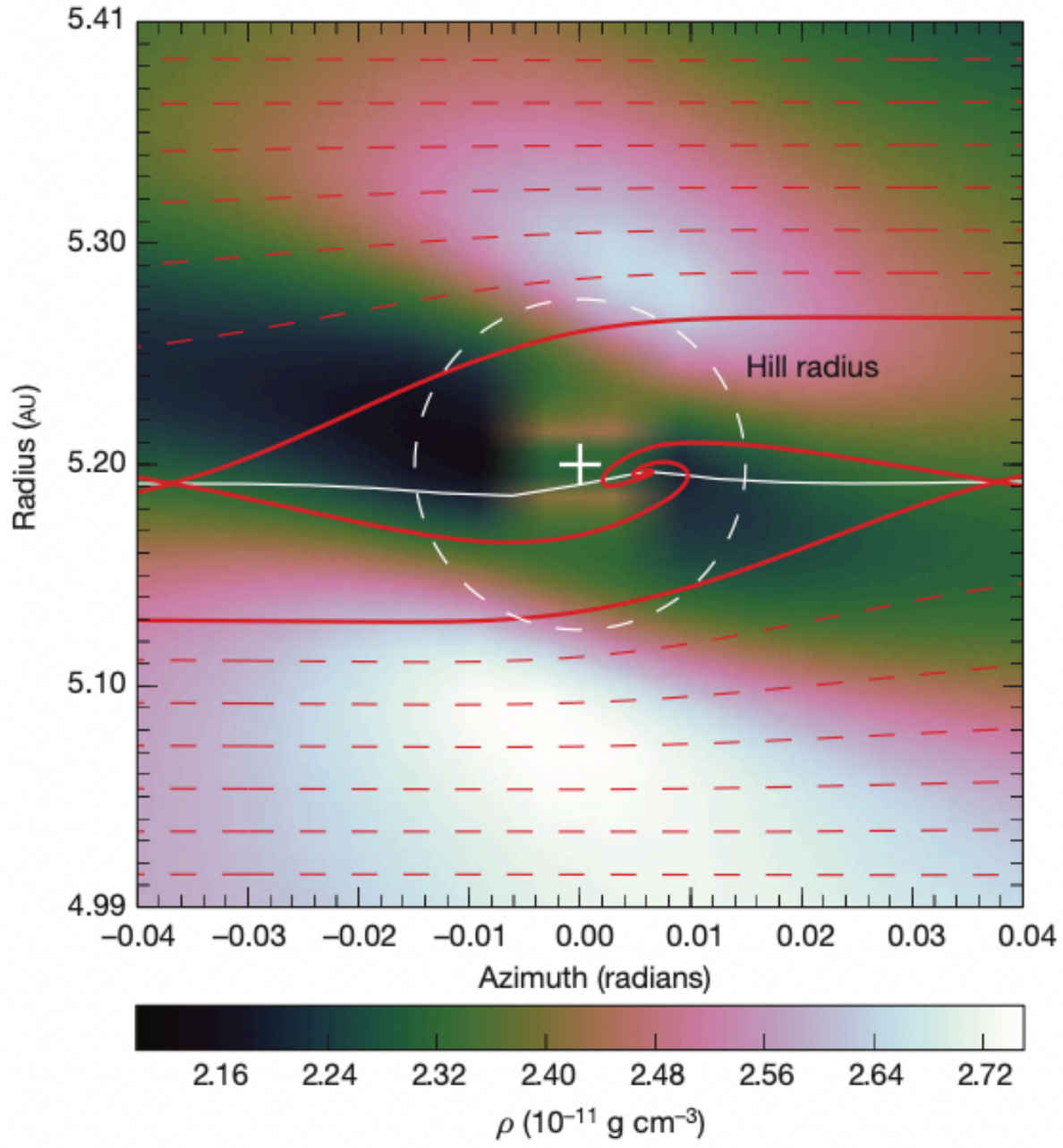

Figure 3 | Density in the vicinity of an irradiating embryo. This equatorial slice of the mass density shows two low-density lobes on each side of the planet (marked with a cross). The more apparent one (left) gives rise to the positive torque. Such lobes are absent for a non-radiating embryo. The dashed circle shows the planetary Hill radius. Streamlines are in red showing the outer limits of the co-orbital region (bold) and paths of material further from the planet (dashed). The white nearly horizontal curve shows corotation, that is, the place where the material is at rest in the planetary frame.

Perturbation due to heat release

midplane temperature

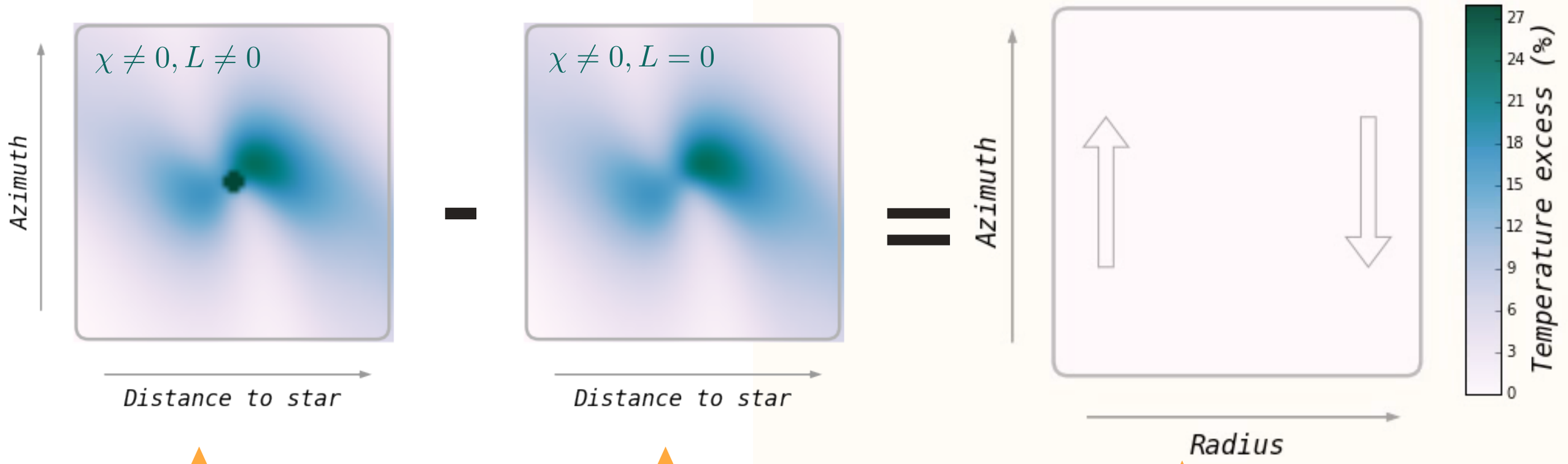

Luminous planet

non-luminous planet

Difference

Net torque

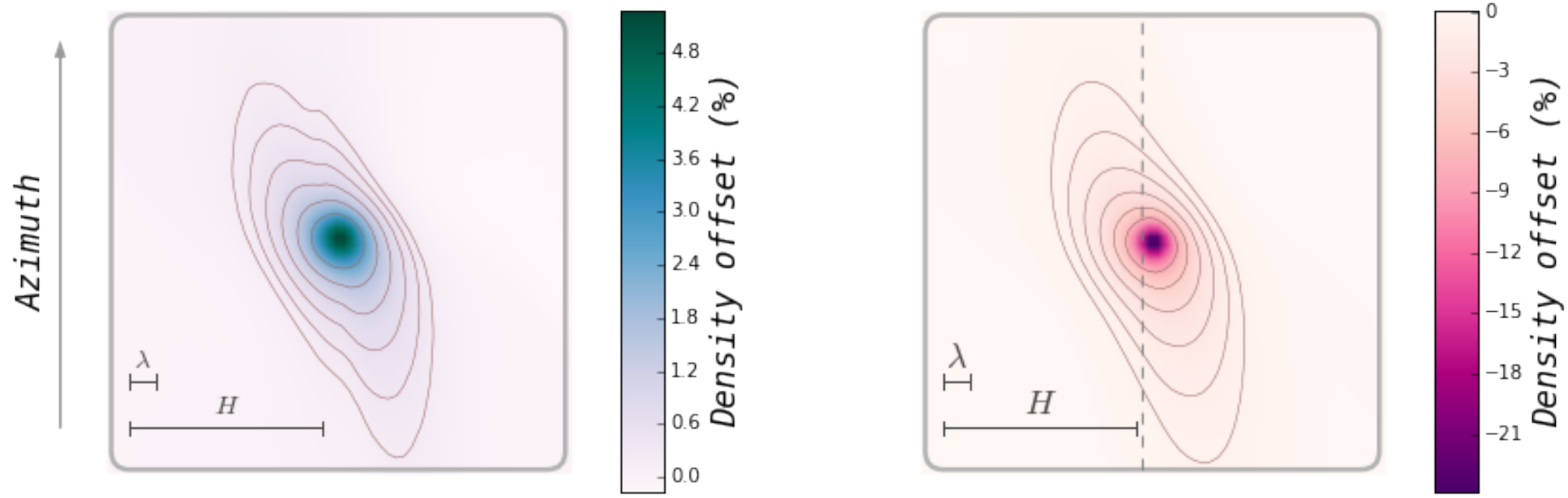

Cold thermal torque ($\propto -L_c$)

Heating torque ($\propto L$)

Torque in adiabatic disc

Torque in disc with thermal diffusion and cold planet

Torque in disc with thermal diffusion and luminous planet

Thermal torque $\propto (L - L_c)$

Numerical study of coorbital thermal torques on cold or hot satellites

Chametla & Masset (2020)

Protoplanetary disc

We consider a three-dimensional, non-self-gravitating inviscid gaseous disc whose motion is governed by the following equations: the equation of continuity which reads

$$\partial_t \rho + \nabla \cdot (\rho \boldsymbol{v}) = 0, \tag{1}$$

the equation of conservation of momentum which reads

$$\partial_t (\rho \boldsymbol{v}) + \nabla \cdot (\rho \boldsymbol{v} \otimes \boldsymbol{v} + p \mathsf{I}) = -\nabla p - \rho \nabla \Phi, \tag{2}$$

and the equation of evolution of the density of internal energy e, which reads

$$\partial_t e + \nabla \cdot (e\boldsymbol{v}) = -p\nabla \cdot \boldsymbol{v} - \nabla \cdot \boldsymbol{F}_H + \boldsymbol{S}. \tag{3}$$

In these equations ρ, $\mathbf{v}$, and Φ denote the density, the velocity, and the gravitational potential, respectively. The source term for the energy (arising from the heat release of the planet) is denoted with $\boldsymbol{S}$ and $\boldsymbol{I}$ represents the unit tensor. Here, $\boldsymbol{F}_H$ is the heat flux, given by

$$\boldsymbol{F}_H = -\chi\rho\nabla\left(\frac{e}{\rho}\right), \tag{4}$$

where χ is the thermal diffusivity.

The gas pressure p obeys the equation of state of ideal gases:

$$p = (\gamma - 1)e, \tag{5}$$

where γ is the adiabatic index.

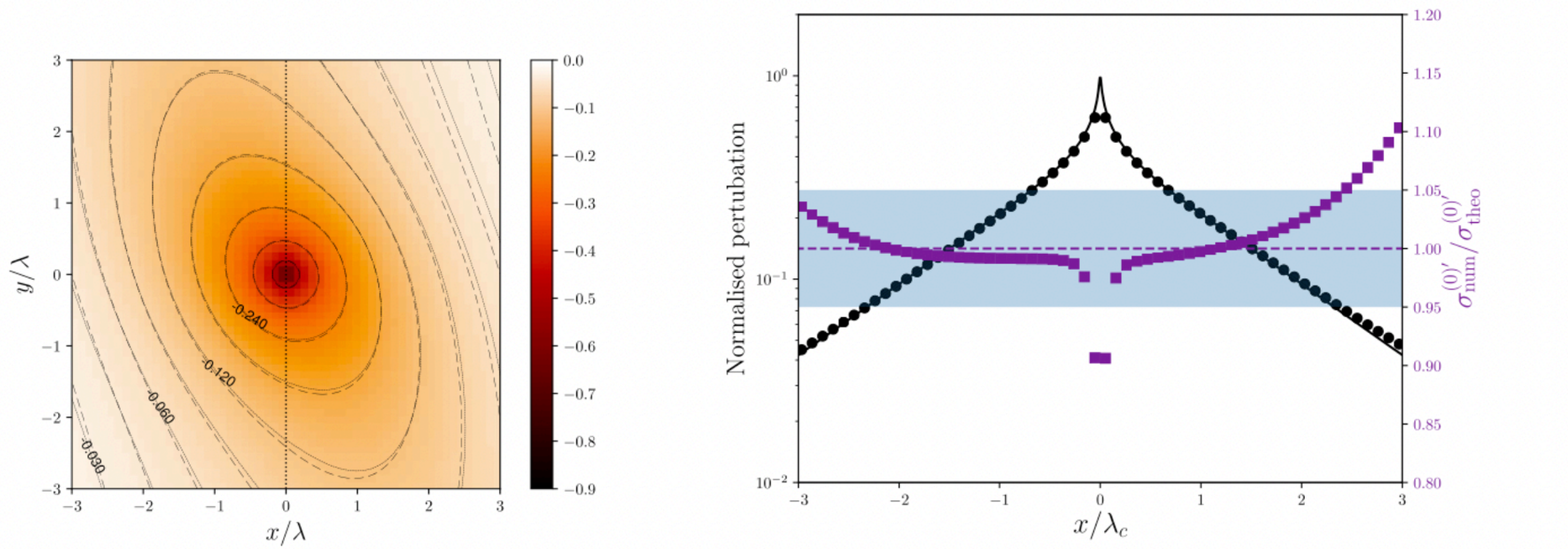

Figure 1. *Left*: Perturbation of surface density $\sigma'^{(0)}$ normalized to $\gamma(\gamma-1)L/\chi c_s^2$. Solid lines: isocontours of the fields obtained after 14 orbital periods of the planet. Dashed lines: Isocontours of the perturbation predicted by linear theory. Here, $x = r - r_p$ and $y = r_p\phi$. This map is obtained by subtracting two runs (a hot one and a cold one) with a planet centred on corotation, as described in Section 4.1. *Right*: Cut of the absolute value of $\sigma'^{(0)}$ along the axis $y = 0$. The black circles represent the values measured in the simulation, while the solid black line represents the value expected from linear theory. The squares (in purple) represent the ratio of the value measured in the numerical simulation to the value expected from linear theory. The light horizontal band delineates the region where these values coincide to within ± 5 per cent.

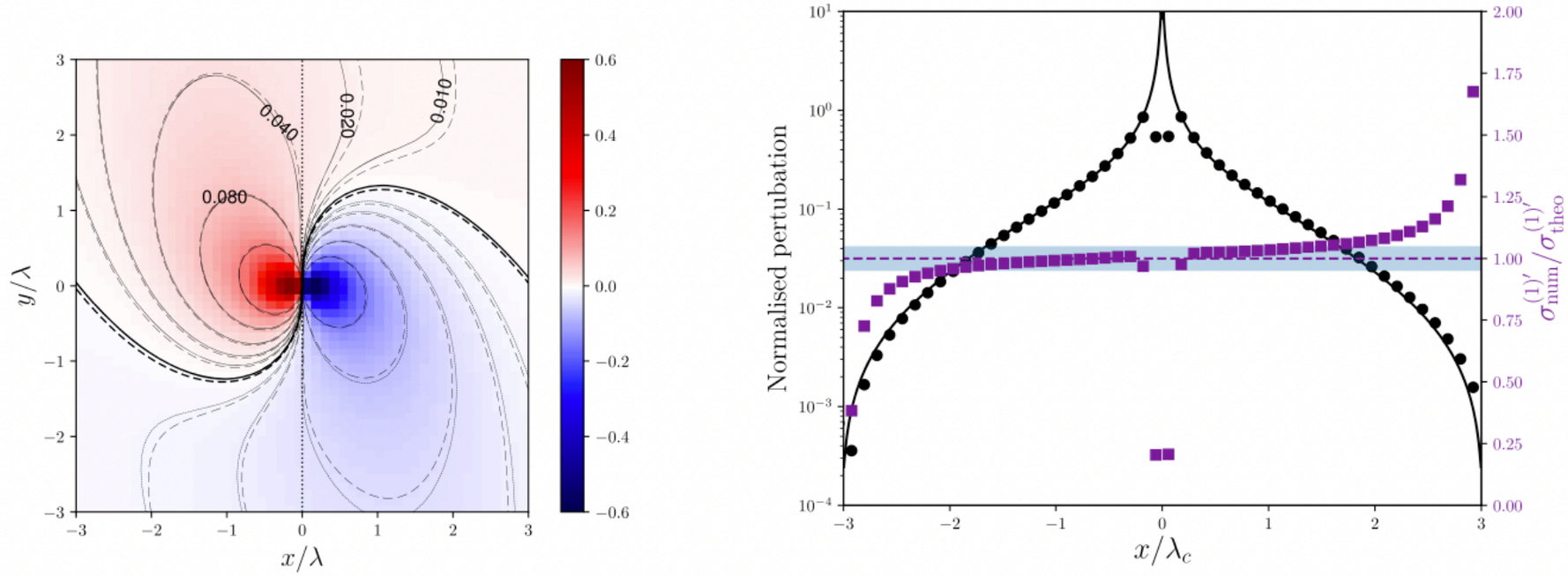

Figure 2. *Left*: Approximation of the partial derivative of the perturbed surface density with respect to x_p, $\sigma'^{(1)}$, normalized to $\gamma(\gamma-1)L/(\chi c_s^2\lambda_c)$. The line style is the same as that of Fig. 1. This map has been obtained using the four runs described in Section 4.2. *Right*: Cut of the absolute value of the map along the $y = 0$ axis. The symbols have same meaning as in Fig. 1. The light horizontal band shows again the region where numerical and theoretical values coincide to within ± 5 per cent.

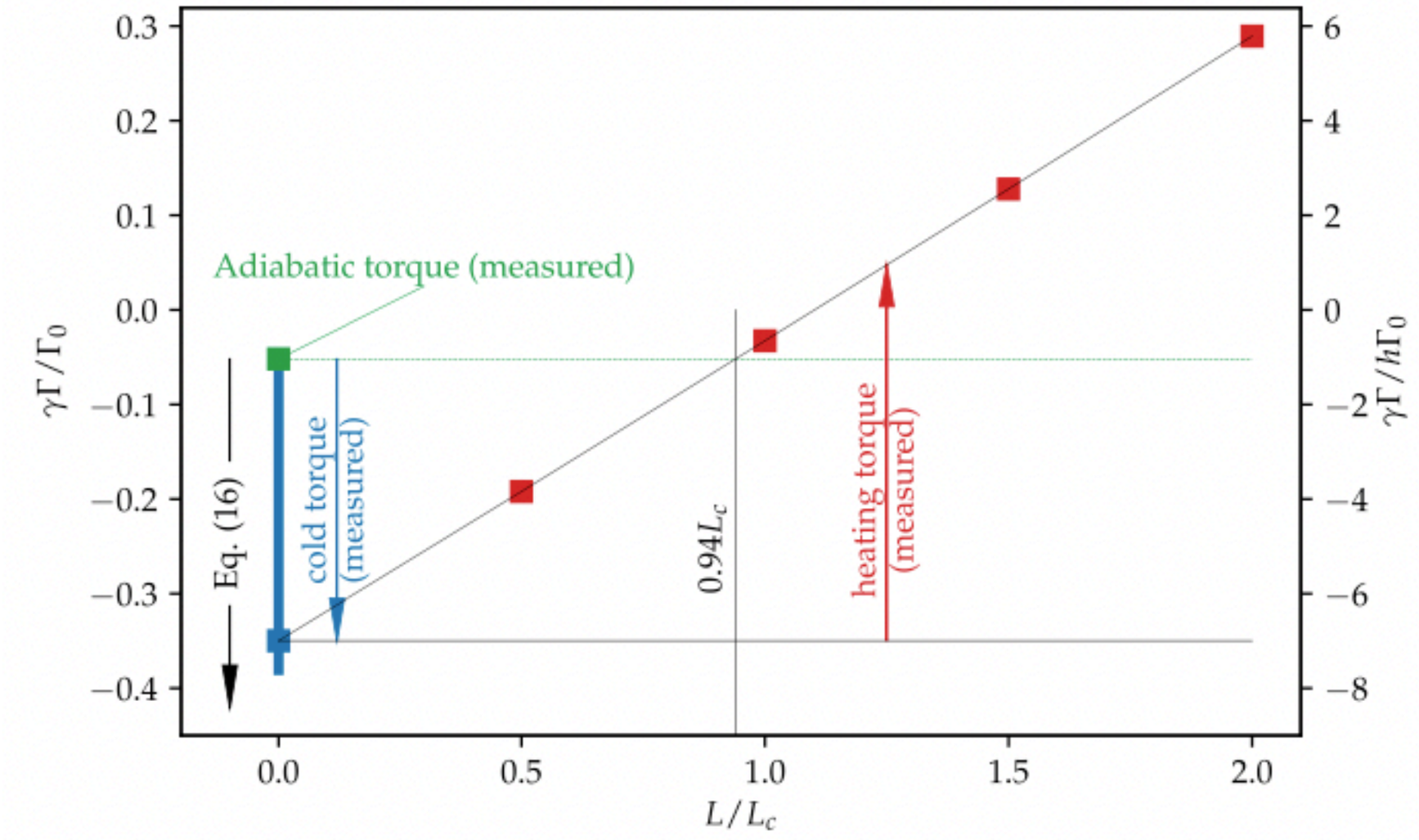

Figure 6. Torque measured in the different runs mentioned in the text (square symbols). The colour matches that of Velasco-Romero & Masset (2019): we use green for adiabatic calculations, blue for cold runs, and red for hot runs.

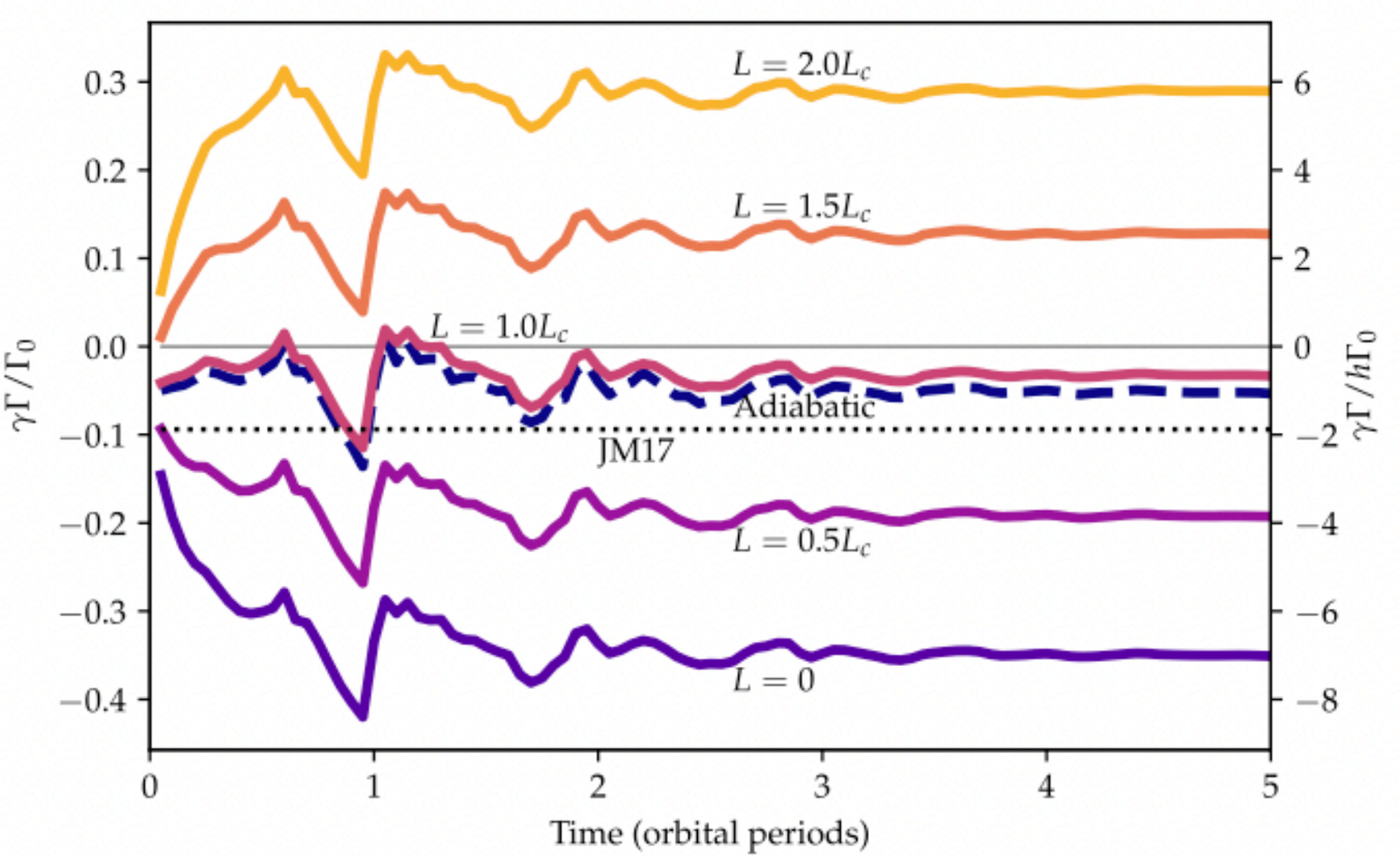

Figure 5. Normalized total torque as a function of time for different cases. The dashed curve shows the torque in the adiabatic disc described in the text. The thick lines show the torque in a disc with similar parameters, except that is has a finite thermal diffusivity, for different planetary luminosities: the bottom curve shows the torque for a non-luminous planet, while the other curves show the torque for a planet of increasing luminosity, from $0.5L_c$ to $2L_c$ by steps of $0.5L_c$, from bottom to top. The horizontal dotted line shows the torque value expected in the adiabatic disc according to Jiménez & Masset (2017). The right vertical axis corresponds to the usual normalization of the torque.

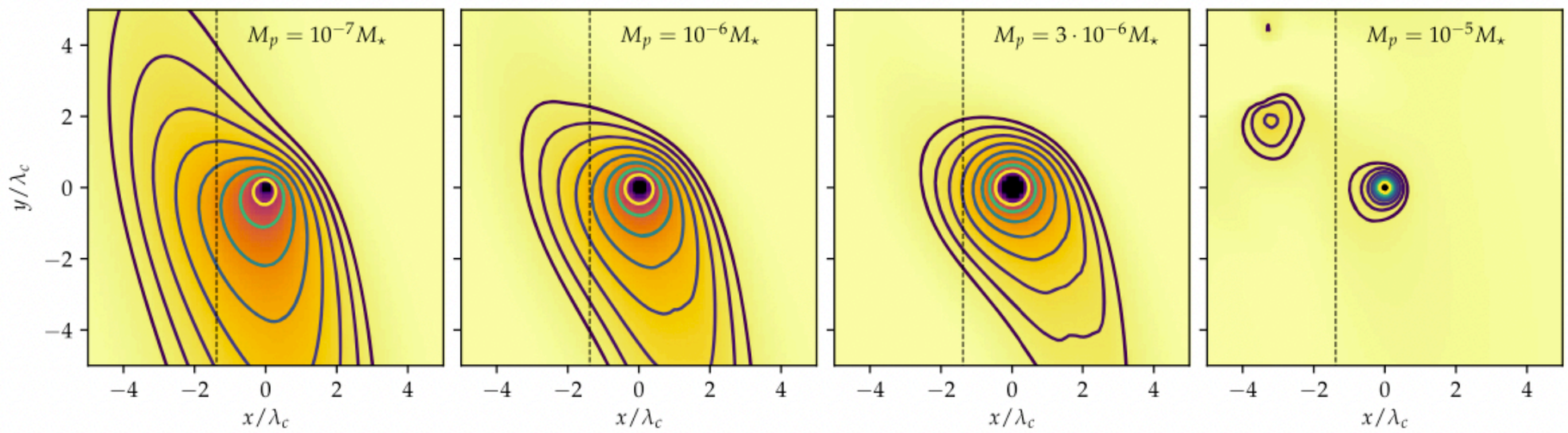

Figure 8. Perturbation of density arising from heat release (obtained by subtracting a hot run and a cold run), integrated in colatitude and normalized to $\gamma(\gamma-1)L/\chi c_s^2$, at $t = 2$ orbits, for the four planet masses considered in the text. The vertical dashed line shows the corotation. The isocontours have same value in the four plots. They start at 0.01 and are in geometric sequence with ratio $\sqrt{2}$.

Hydrodynamical simulations plus dust particles including **Dust turbulent diffusion** (Chametla et al. 2021):

$$D_d = \nu \frac{1 + 4St^2}{(1 + St^2)^2}$$

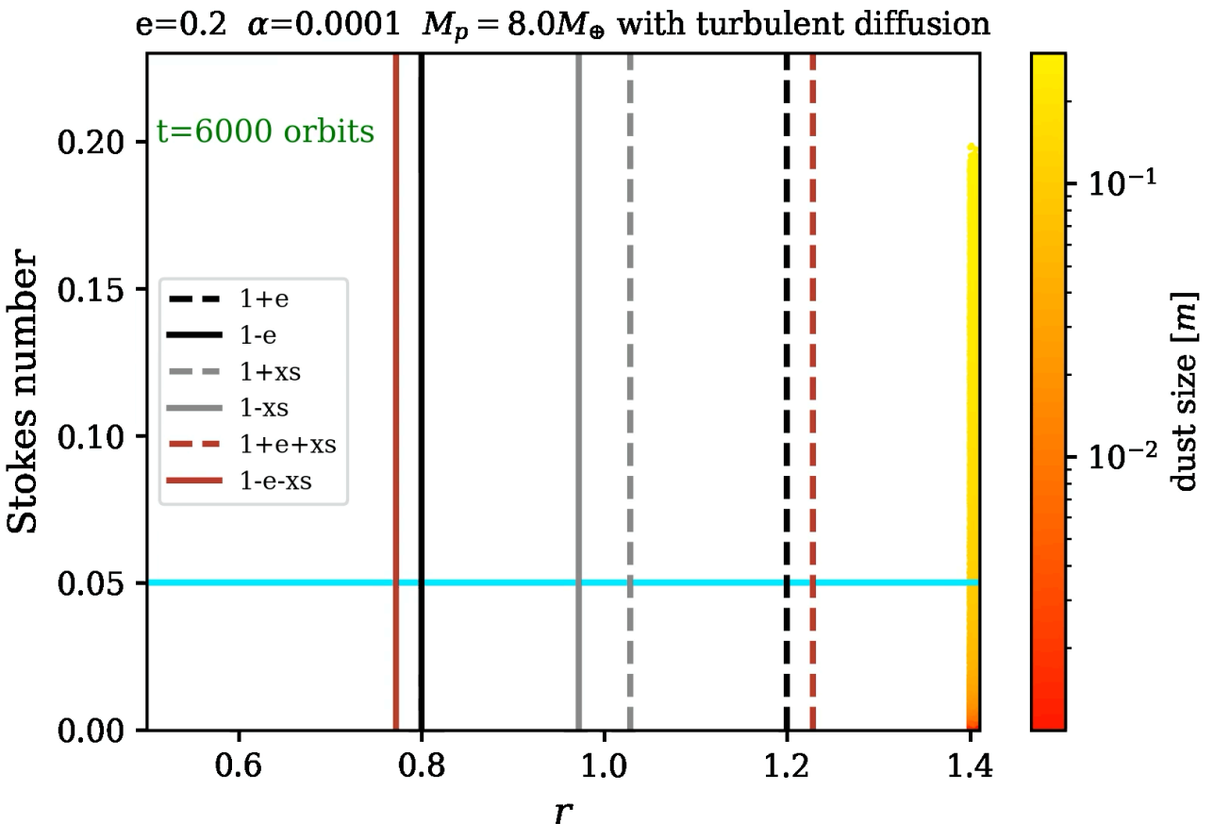

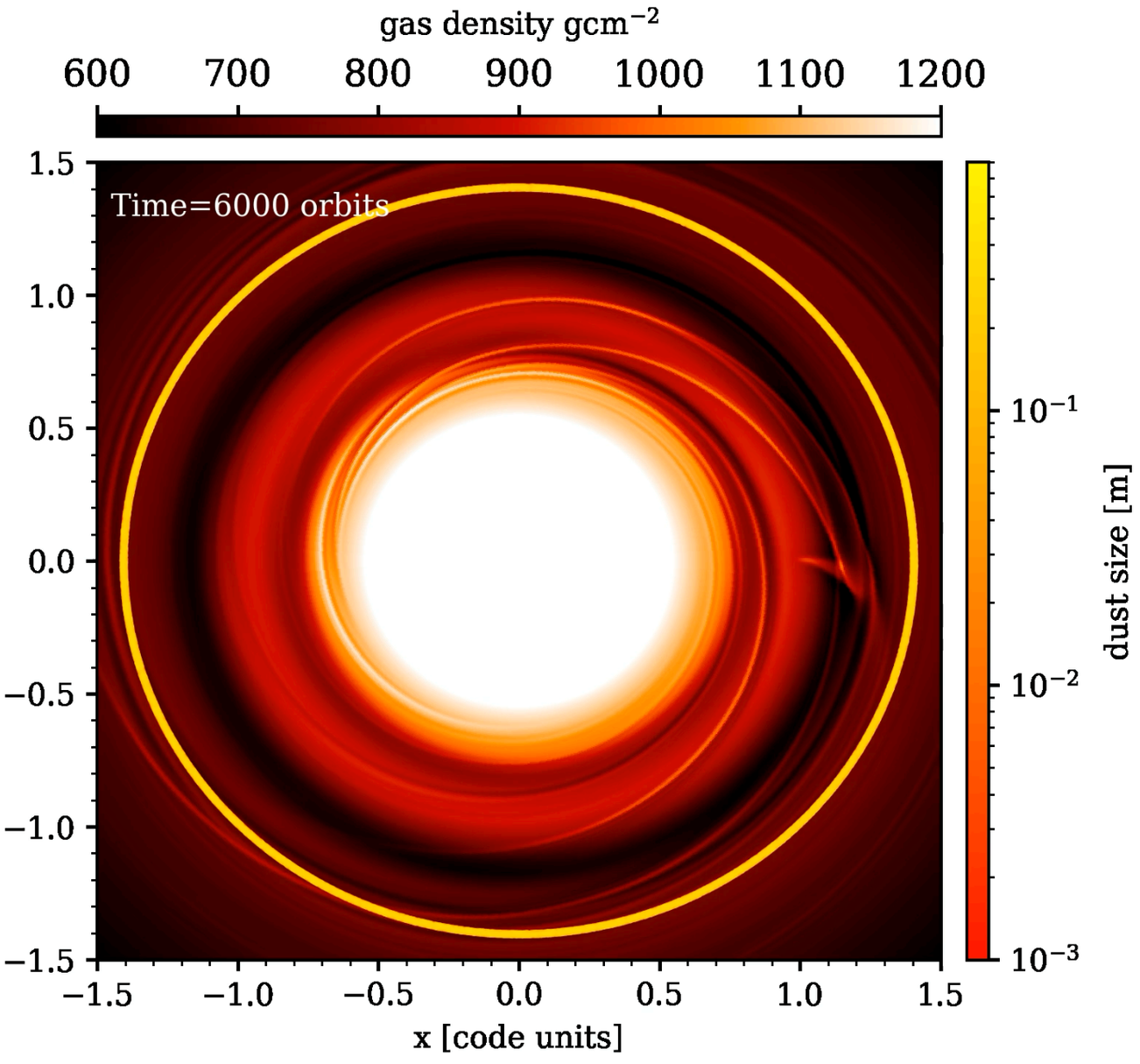

Migration type II: Simulations

Numerical simulations (Crida et al 2006) have led to the following approximate combined gap opening criterion:

$$P = \frac{3}{4}\frac{H}{R_H} + \frac{50}{q\mathscr{R}} \leq 1$$

where $\mathscr{R} \equiv \dfrac{\Omega_p a^2}{\nu}$ is the Reynolds number.

$P > 1$

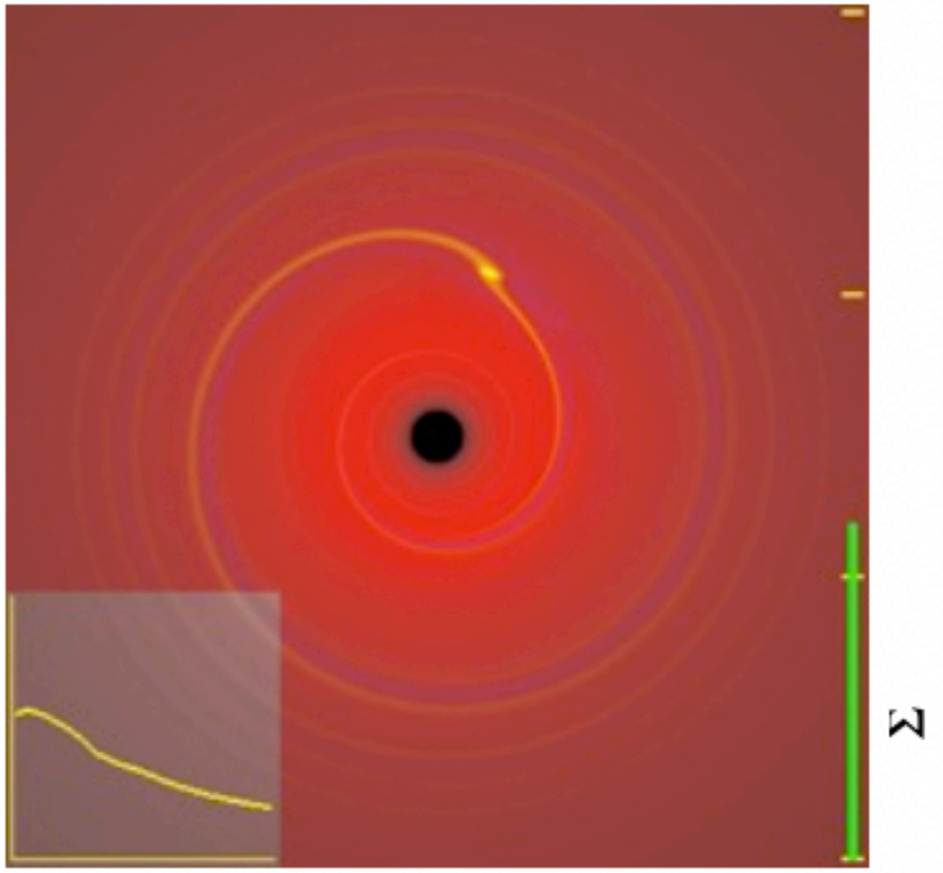

$P \leq 1$

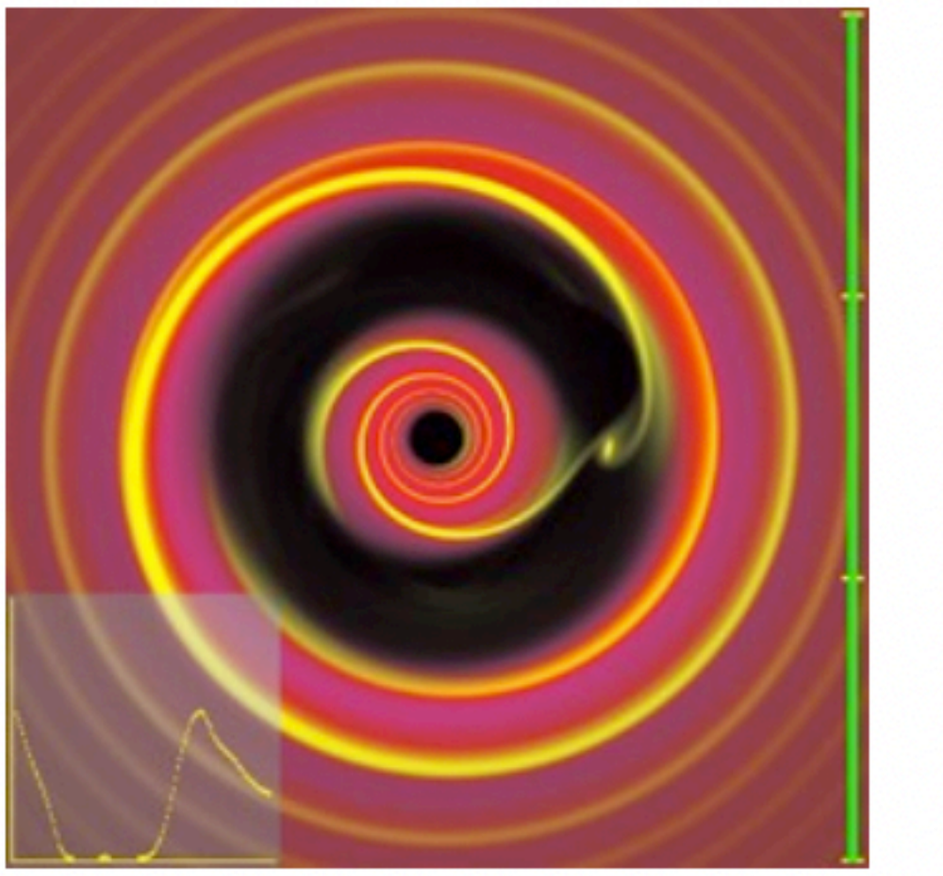

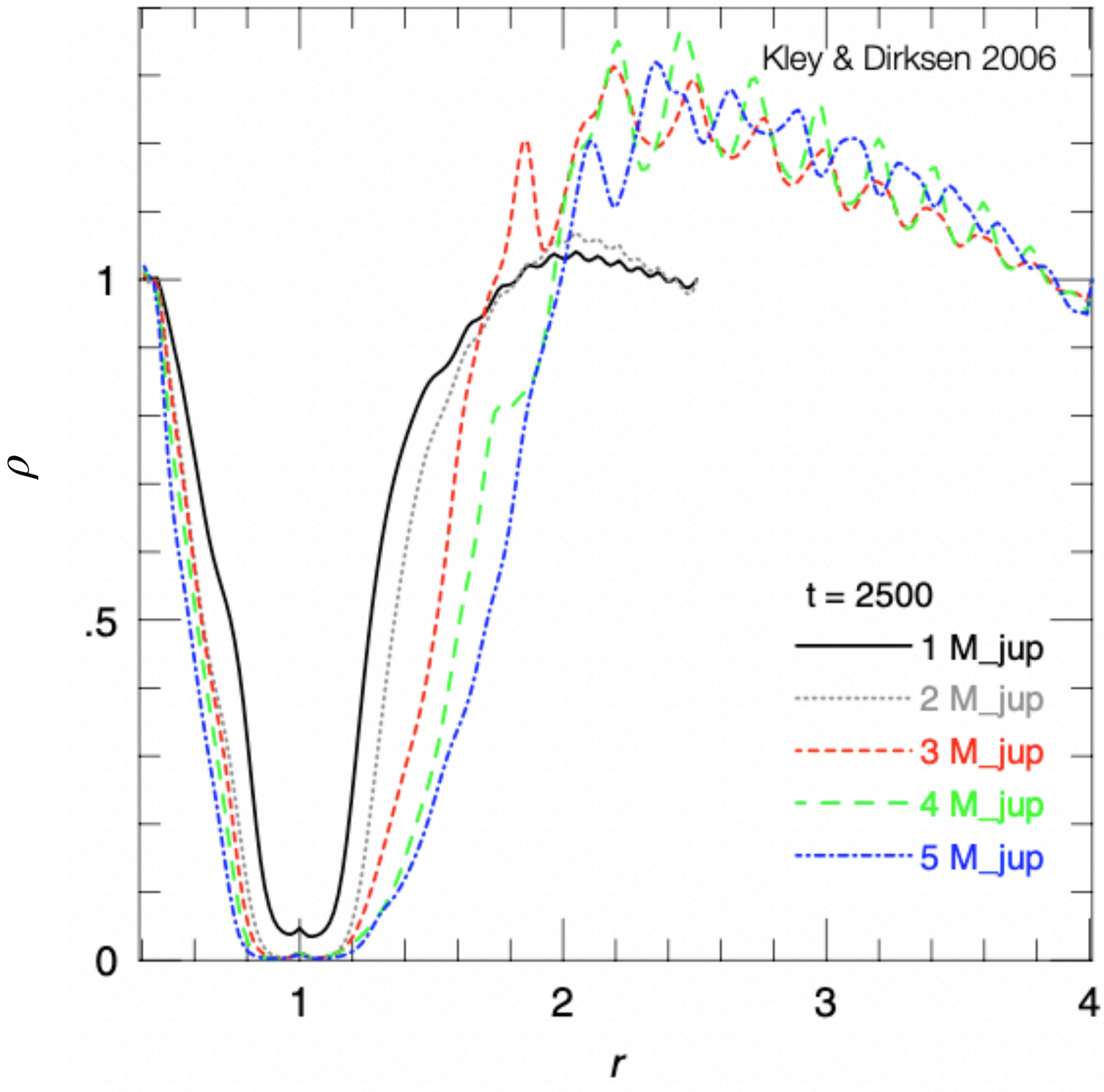
Kley & Dirksen 2006
ρ
1
.5
0
1
2
3
4
r
t = 2500
1 M_jup
2 M_jup
3 M_jup
4 M_jup
5 M_jup

Gaps formed in disks without embedded planets

The equations are

$$\frac{\partial \rho}{\partial t} + \nabla \cdot (\rho \boldsymbol{v}) = 0, \tag{1}$$

$$\frac{\partial \rho \boldsymbol{v}}{\partial t} + \nabla \cdot \left[\rho \boldsymbol{v}\boldsymbol{v}^{\mathrm{T}} - \boldsymbol{B}\boldsymbol{B}^{\mathrm{T}}\right] + \nabla P_{\mathrm{t}} = -\rho \nabla \Phi, \tag{2}$$

$$\frac{\partial E}{\partial t} + \nabla \cdot [(E + P_{\mathrm{t}})\boldsymbol{v} - (\boldsymbol{v} \cdot \boldsymbol{B})\boldsymbol{B}] = -\rho \boldsymbol{v} \cdot \nabla \Phi - \nabla \cdot [(\eta \cdot J) \times B], \text{ and} \tag{3}$$

$$\frac{\partial B}{\partial t} + \nabla \times (\boldsymbol{v} \times \boldsymbol{B}) = -\nabla \times (\eta \cdot J) \tag{4}$$

with the gas density ρ, the velocity vector $\boldsymbol{v}$, the magnetic field vector $\boldsymbol{B}$, the total pressure $P_{\mathrm{t}} = P + 0.5B^2$, the gravitational potential Φ, the total energy $E = \rho\epsilon + 0.5\rho\boldsymbol{v}^2 + 0.5\boldsymbol{B}^2$ with the internal energy $\rho\epsilon = P/(\Gamma - 1)$, the current density $J = \nabla \times B$, and the Ohmic resistivity η. We considered Ohmic diffusion.

Model name	$N_r \times N_\theta \times N_\phi$	Δr [AU]:$\Delta\theta$ [rad]:$\Delta\phi$ [rad]	D2G	Inner orbits	$\langle\alpha\rangle$	$\langle\Sigma'\rangle$
`D2G_e-4`	$256 \times 128 \times 512$	$20\text{–}100{:}0.72{:}2\pi$	10^{-4}	800	0.013	0.04
`D2G_e-2`	$256 \times 128 \times 512$	$20\text{–}100{:}0.72{:}2\pi$	10^{-2}	1045	0.003	0.09
Disk parameter		Stellar parameters				
$M_{\rm total} \cong 0.085\ M_*$	$\Sigma_0 = 5.94\ {\rm g\ cm^{-2}}\ \frac{100\ {\rm AU}}{R}$	$T_* = 4000$ K	$0.95\ L_\odot$	$M_* = 0.5\ M_\odot$	spectral type ~K	

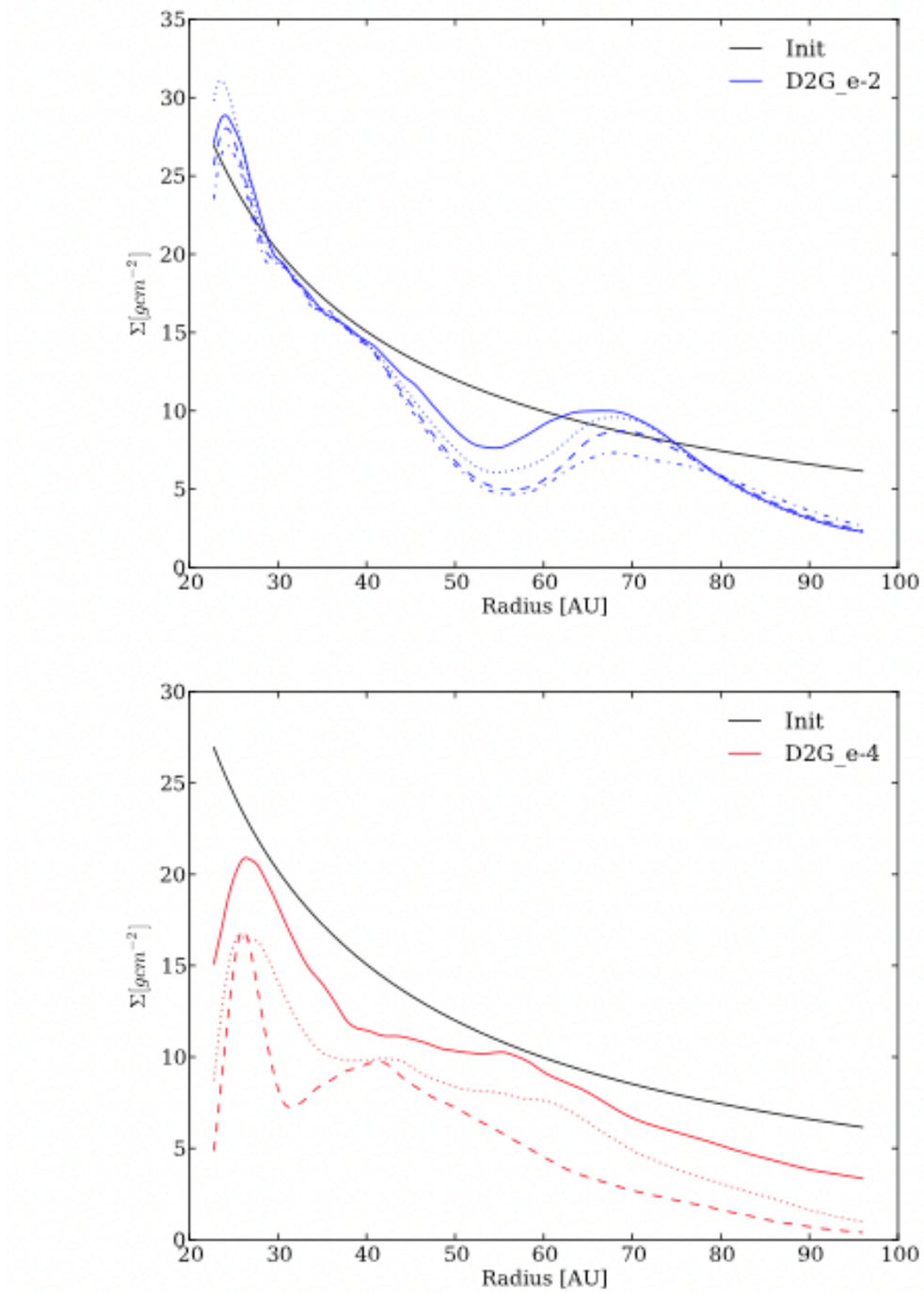

Fig. 2. Radial surface density profiles, plotted in steps of 200 inner orbits, from initial (black solid) to final (solid, dotted, dashed, and dashed-dotted) for model `D2G_e-2` (blue) and model `D2G_e-4` (red).

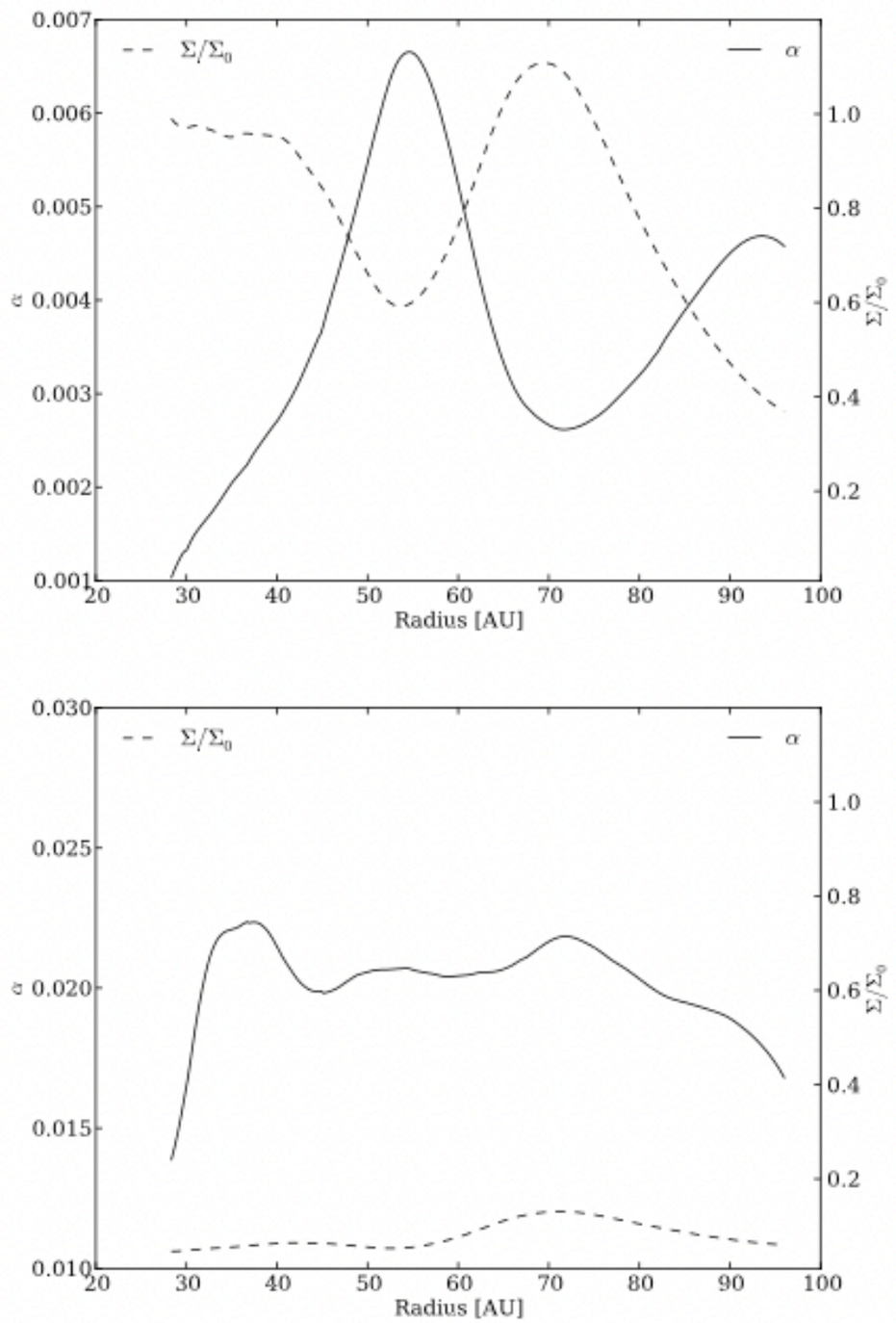

Fig. 3. Time-averaged radial profile of the accretion stress α (solid line) and the normalized surface density Σ/Σ_0 (dashed line) for models `D2G_e-2` (*top*) and `D2G_e-4` (*bottom*).

Flock et al. (2015)

Gaps formed by MRI

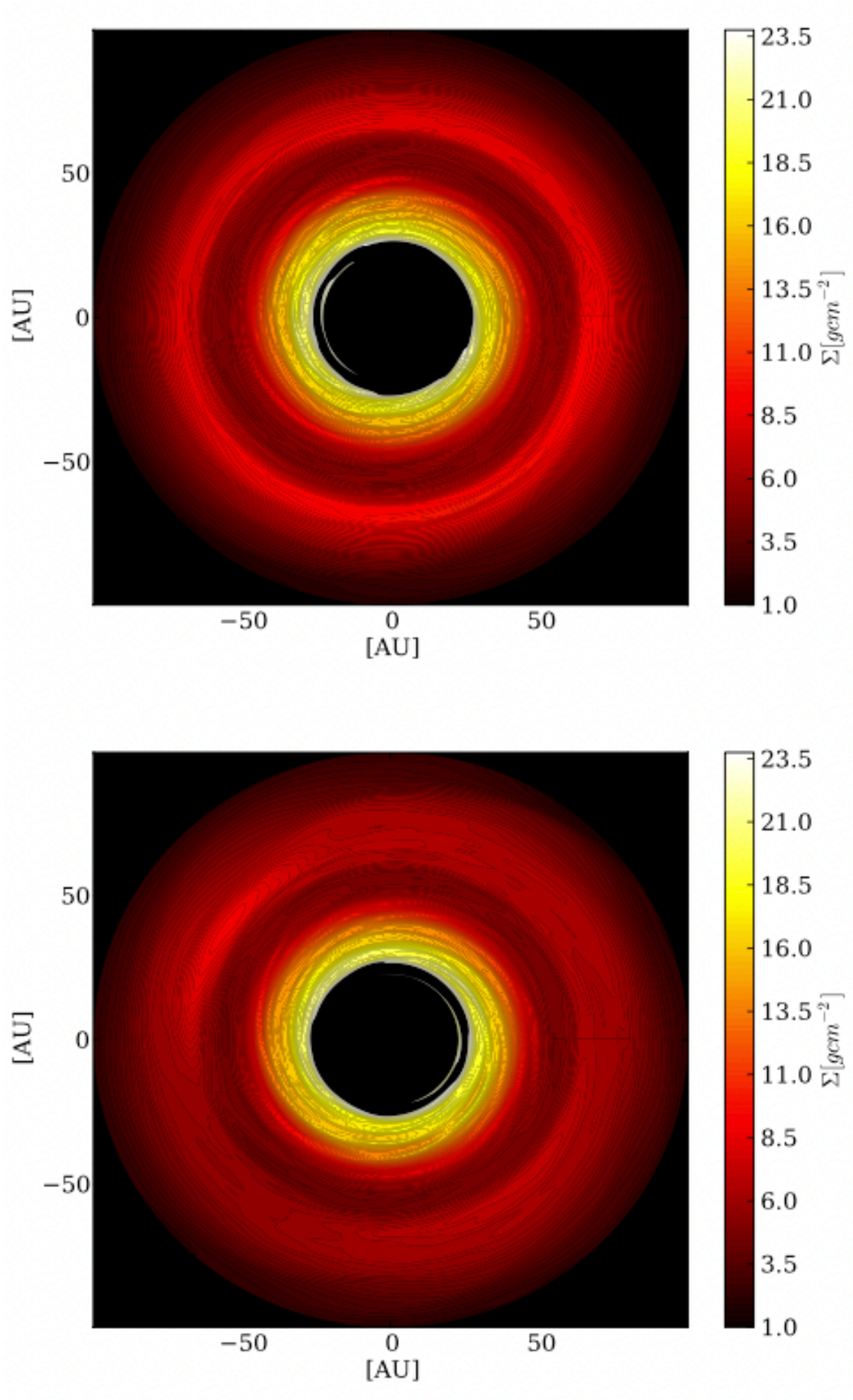

Turbulent stress within dead zones and magnetic field dragging induced by Rossby vortices

Chametla et al. (2023)

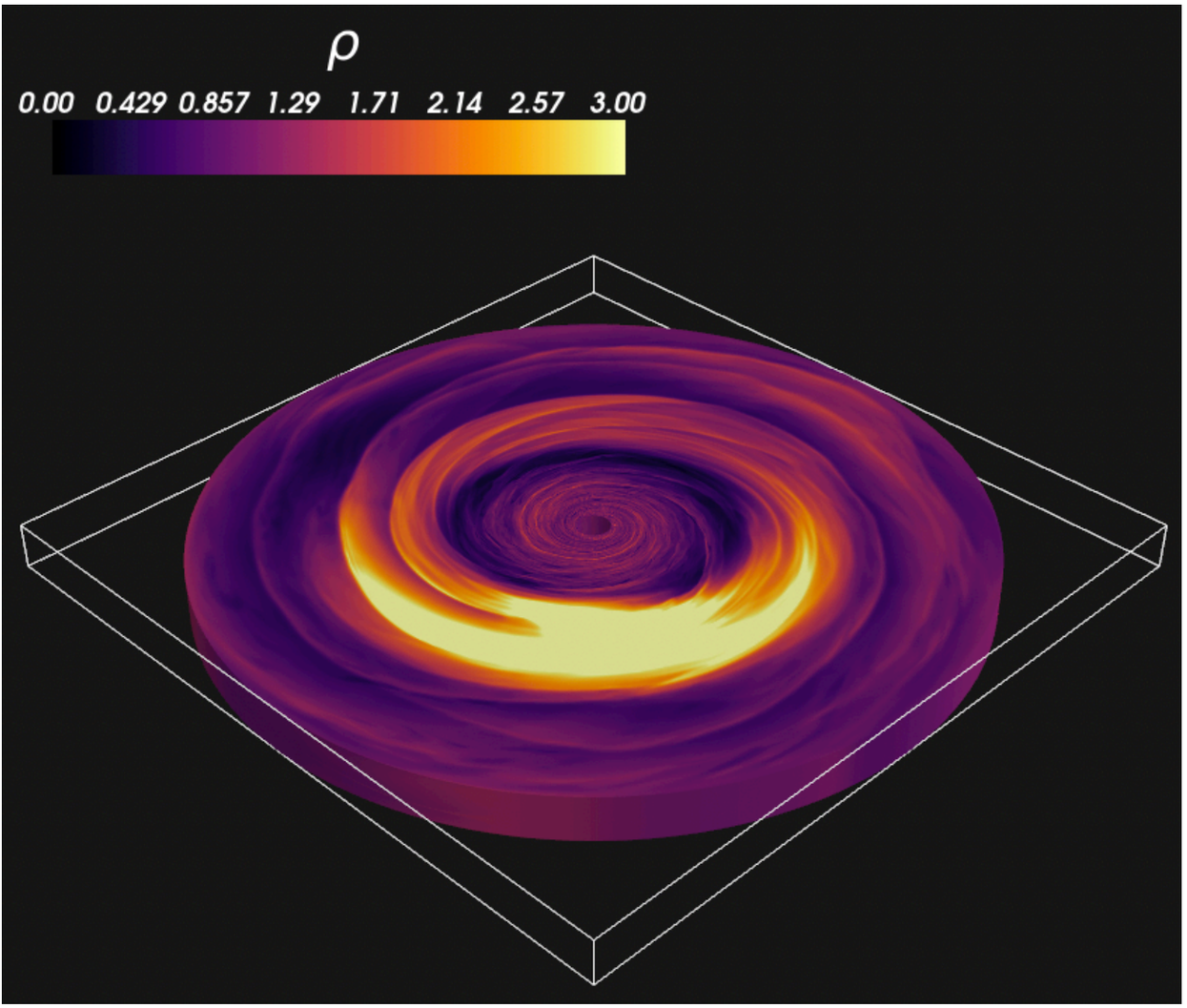

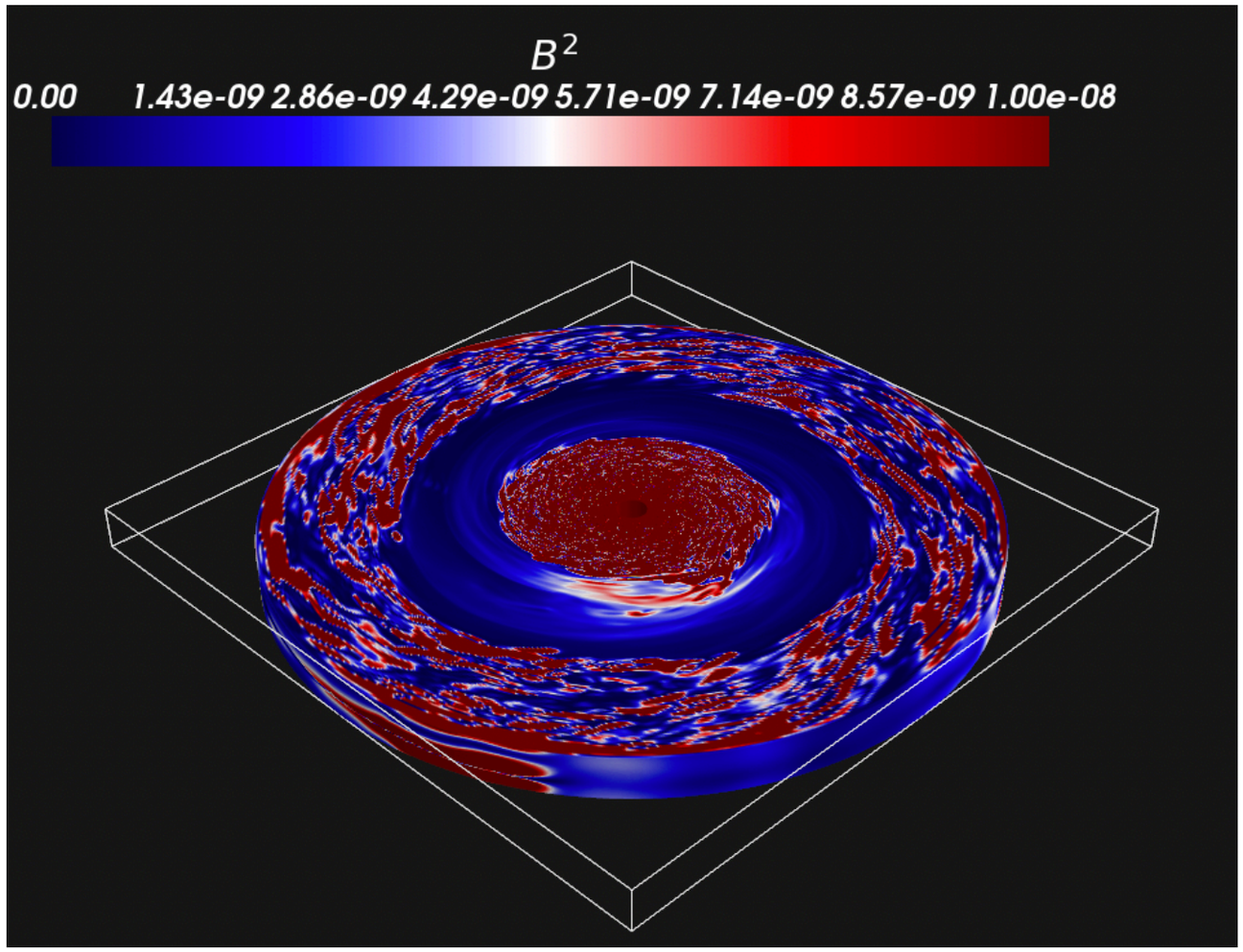

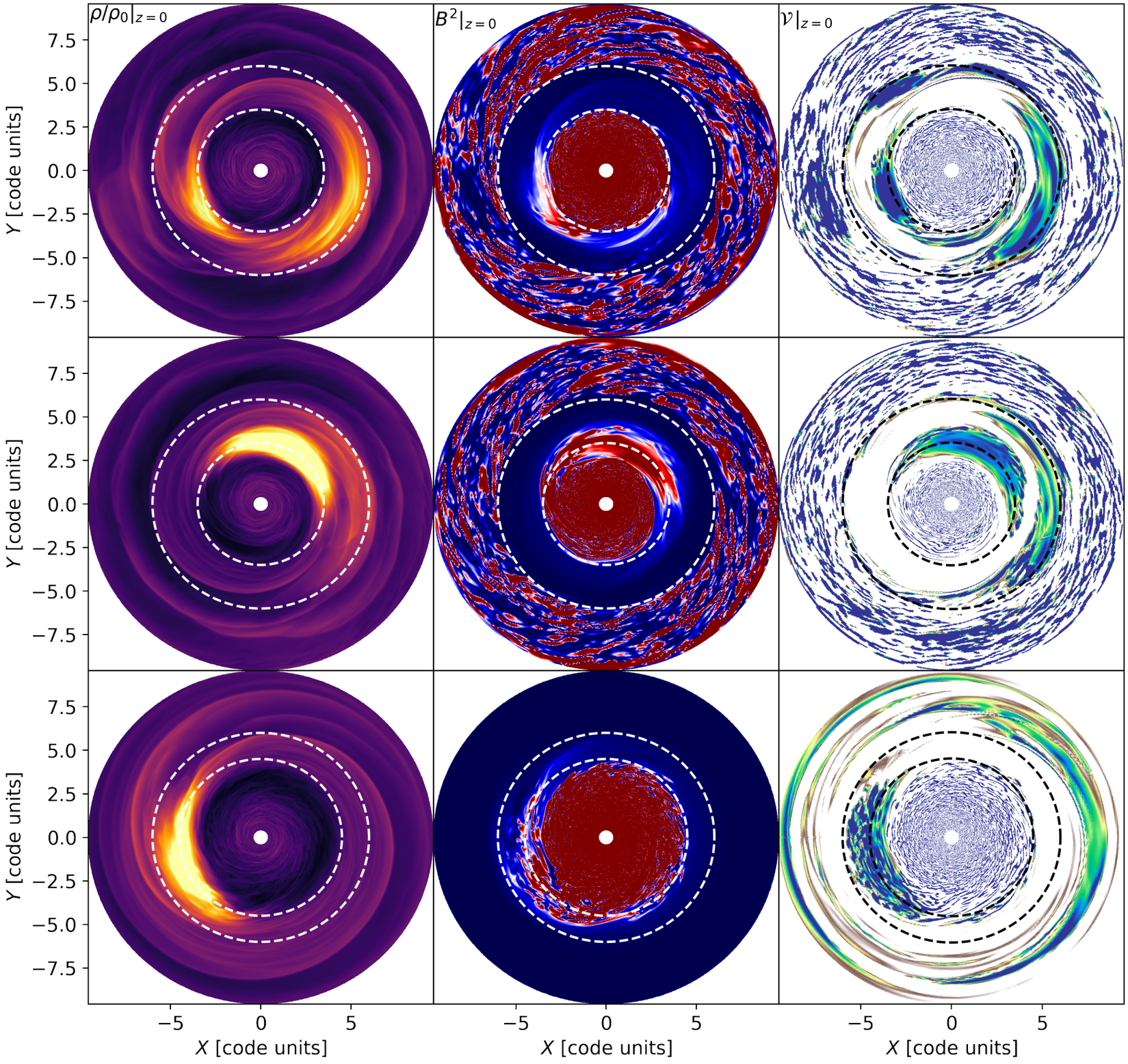
$\rho/\rho_0|_{z=0}$
$B^2|_{z=0}$
$\mathcal{V}|_{z=0}$
Y [code units]
X [code units]
7.5
5.0
2.5
0.0
−2.5
−5.0
−7.5
−5
0
5

Planets outside the gaps

Low-mass planets falling into gaps can survive inward migration

Raúl O. Chametla [1] and F. Javier Sánchez-Salcedo [2]

Governing equations

We consider a 3D non-self-gravitating gas disc whose evolution is governed by the following equations:

$$\partial_t \rho + \nabla \cdot (\rho \mathbf{v}) = 0, \tag{1}$$

$$\partial_t (\rho \mathbf{v}) + \nabla \cdot (\rho \mathbf{v} \otimes \mathbf{v} + p \mathsf{I}) = -\nabla p - \rho \nabla \Phi, \tag{2}$$

where ρ and $\mathbf{v}$ denote the density and velocity of the gas, respectively. Furthermore, Φ denotes the gravitational potential, I is the unit tensor, and p is the gas pressure. For the latter, we consider the globally isothermal equation of state

$$\nu = \alpha c_s H \tag{9}$$

with

$$\alpha = \alpha_0 \left\{ 1 + \frac{1}{2} \left[\tanh\left(\frac{r - r_1}{h_1} \right) - \tanh\left(\frac{r - r_2}{h_2} \right) \right] \right\}^{-1}. \tag{10}$$

In Eq. (10) $\alpha_0 = 10^{-3}$.

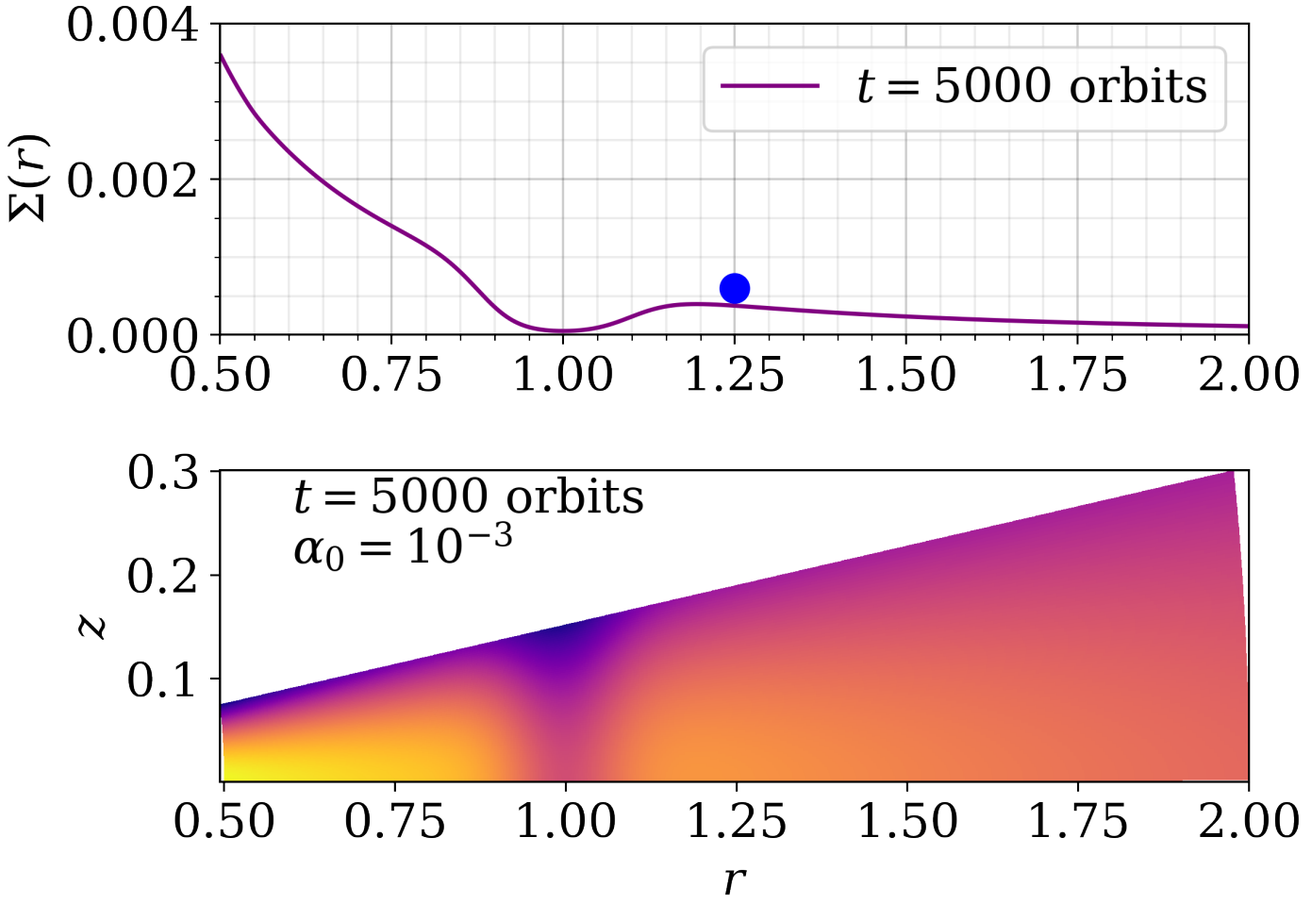

Table 1. Initial conditions and main parameters of our simulations (r_0 denotes a reference radius*).

	Parameter	Value [code units]
	Central star	
Mass of the star	$M_\star$	1.0
	Disk	
Aspect ratio at r_0	h	0.05
Surface density at r_0	Σ_0	6.3662×10^{-4}
Surface density slope	σ	1.0
Temperature slope	β	0.0
α-viscosity	α_0	1×10^{-3}
	Planet	
Planet mass interval	M_p	$[3 \times 10^{-6}, 1.5^{-5}]$
Planet location	(r_p, ϕ_p, θ_p)	$(1, 0, 0)$
Softening length	ϵ	$0.1H(r_p)$
	Global mesh	
Radial extension	r	$[0.5, 2.0]$
Azimuthal extension	ϕ	$[0, 2\pi]$
Polar extension	θ	$[\frac{\pi}{2} - 3h, \frac{\pi}{2}]$
Radial resolution	N_r	768 cells
Azimuthal resolution	N_ϕ	3200 cells
Polar resolution	N_θ	76 cells
Radial spacing	A	Aritmethic
	Additional parameters	
Reference frame	C	Corotating
Frame angular speed	$\Omega(r_p)$	Ω_p
Gravitational constant	G	1.0
Orbital period at r_p	T_0	$2\pi\Omega_p^{-1}$

NOTE—*We consider $r_0 = 5.2$ au and $M_\star = 1 M_\odot$ when scaling back to physical units.

1e−7
$M_p = 1M_\oplus$
$d\mathcal{T}/dM$
r
1e−7
$M_p = 3M_\oplus$
$d\mathcal{T}/dM$
r
1e−7
$M_p = 5M_\oplus$
$d\mathcal{T}/dM$
r
1e−6
$M_p = 7M_\oplus$
$d\mathcal{T}/dM$
r
1e−6
$M_p = 10M_\oplus$
$d\mathcal{T}/dM$
r
1e−6
$M_p = 15M_\oplus$
$d\mathcal{T}/dM$
r

Total torque

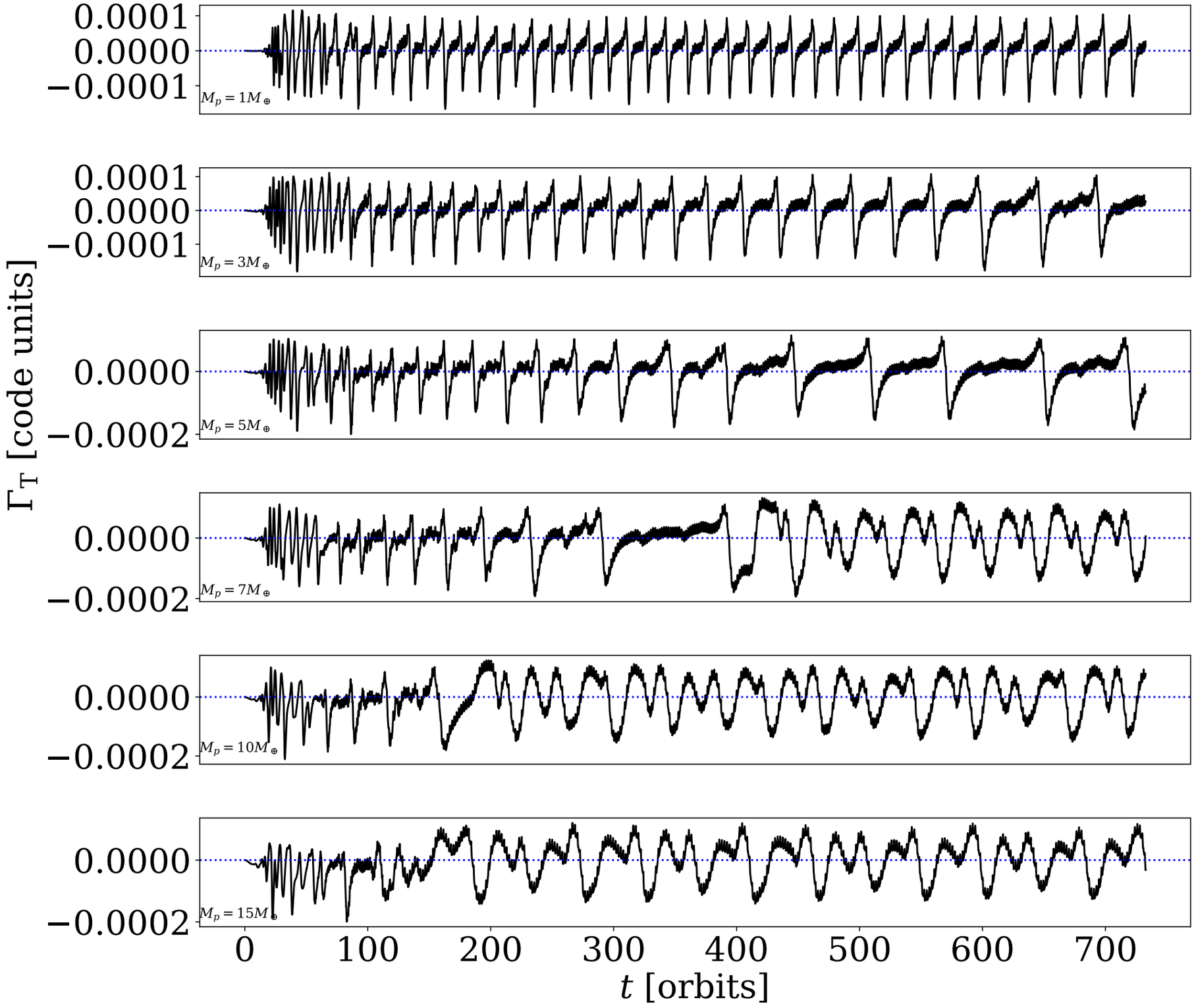

Planet migration becomes stagnant near the edge of the gap!

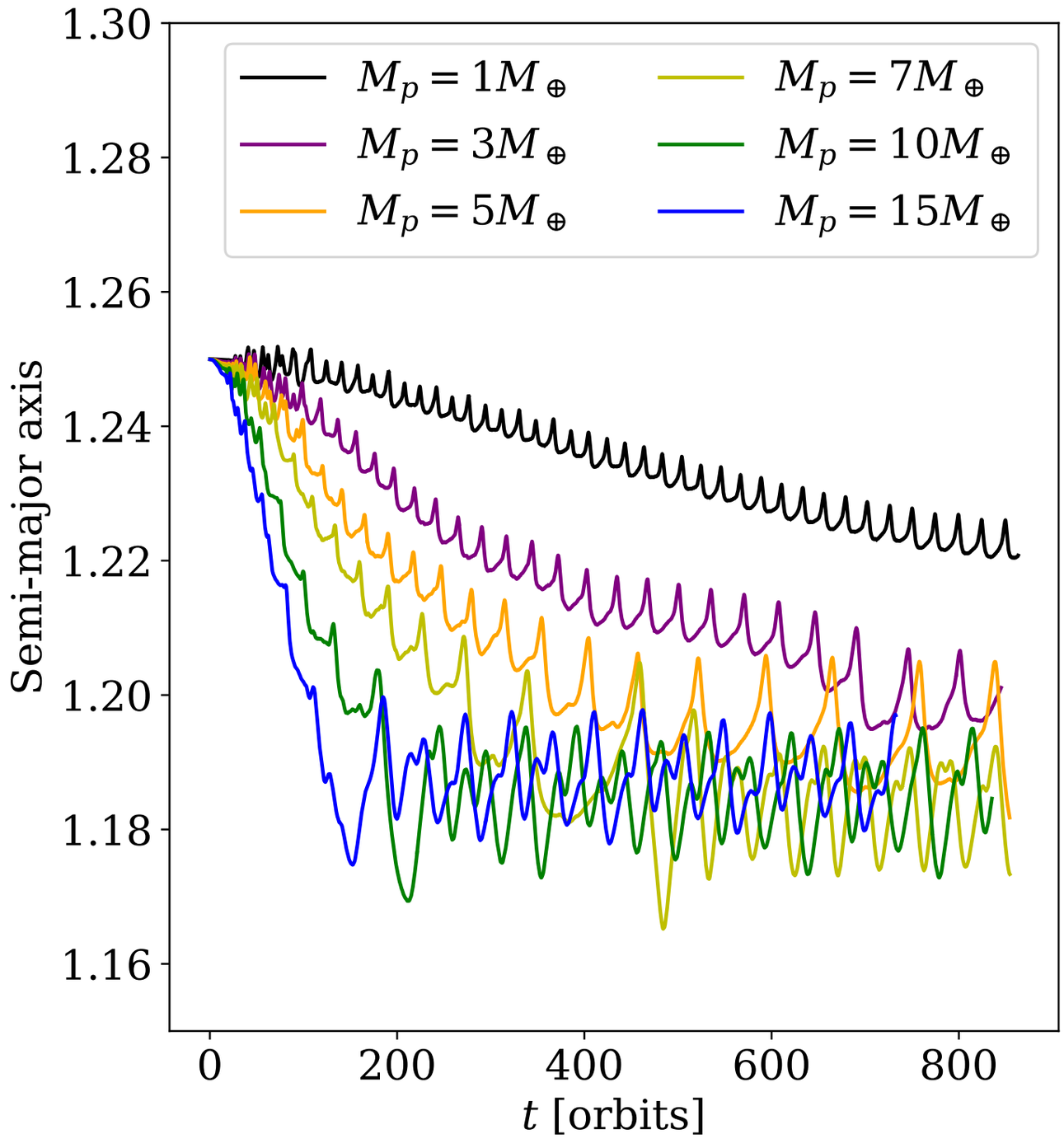

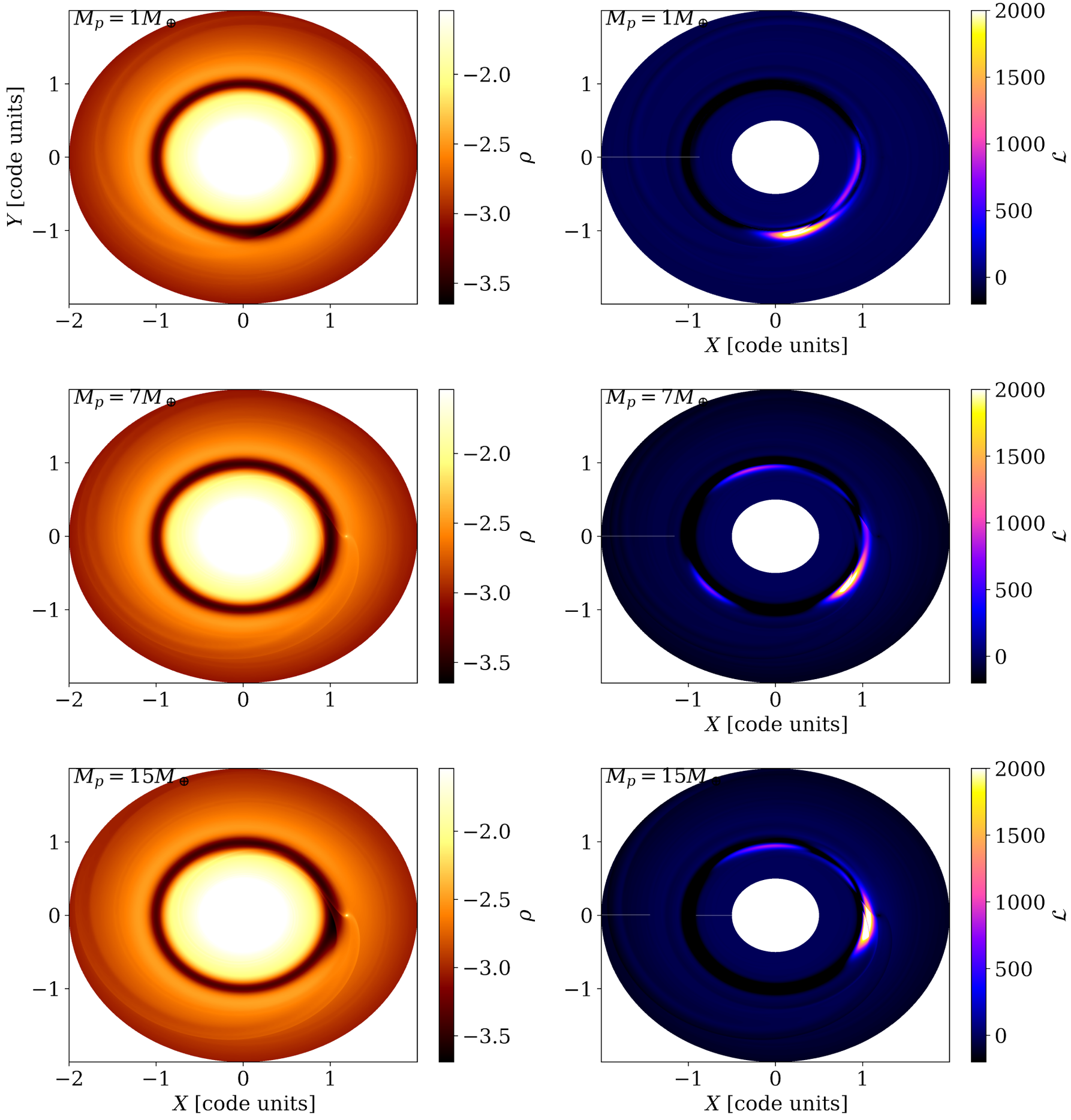
$M_p = 1M_\oplus$
$M_p = 1M_\oplus$
$M_p = 7M_\oplus$
$M_p = 7M_\oplus$
$M_p = 15M_\oplus$
$M_p = 15M_\oplus$
Y [code units]
X [code units]
ρ
$\mathcal{L}$
−2.0
−2.5
−3.0
−3.5
2000
1500
1000
500
0
−2
−1
0
1

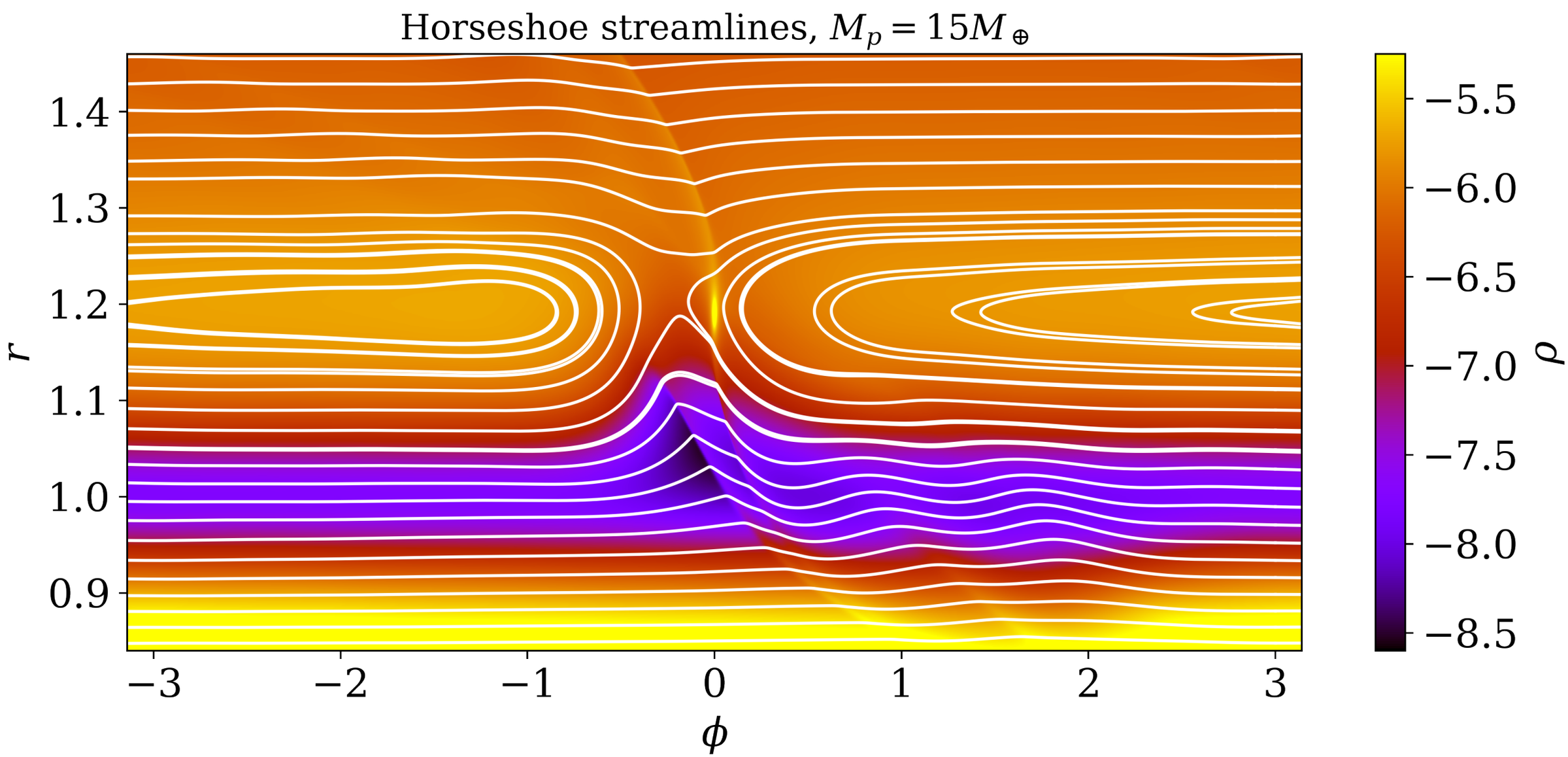
Horseshoe streamlines, $M_p = 15 M_\oplus$
1.4
1.3
1.2
1.1
1.0
0.9
r
−3
−2
−1
0
1
2
3
ϕ
−5.5
−6.0
−6.5
−7.0
−7.5
−8.0
−8.5
ρ